THE UNIVERSITY OF MANITOBA

ON THE APPLICATION OF FOURIER EXPANSION TO ELASTO-PLASTIC FINITE ELEMENT STRESS ANALYSIS

by

Ray, Ruey-yau Wu

A THESIS

SUBMITTED TO THE FACULTY OF GRADUATE STUDIES

IN PARTIAL FULFILLMENT OF THE REQUIREMENTS FOR THE DEGREE

OF MASTER OF SCIENCE

DEPARTMENT OF MECHANICAL ENGINEERING

WINNIPEG, MANITOBA

APRIL, 1977

"ON THE APPLICATION OF FOURIER EXPANSION

TO ELASTO-PLASTIC FINITE ELEMENT STRESS ANALYSIS"

by

RAY, RUEY-YAU WU

A dissertation submitted to the Faculty of Graduate Studies of the University of Manitoba in partial fulfillment of the requirements of the degree of

MASTER OF SCIENCE

ABSTRACT

The work in this thesis presents a preliminary study on the application of Fourier expansion to the three-dimensional elasto-plastic finite element stress analysis. Problems of axisymmetric solids subject to non-axisymmetric loads are attempted by a combined Fourier expansion and finite element method.

Based on the analysis, two computer codes entitled " NLSTRS " and " NTEPSA " have been written to incorporate the elastic and elasto-plastic material behavior respectively. It is found that this combined method affords a complete and accurate set of solutions for the elastic analysis of axisymmetric solids. For the elasto-plastic analysis, the method is somewhat restricted from applications of general loading conditions because of the tremendous amount of computer effort involved in handling mode-mixing problems. However, it is still a competitive method for problems of non-axisymmetric loads which can be described by limited number of modes.

ACKNOWLEDGEMENT

I would like to express my deep appreciation to Dr. T. R. Hsu for his continuing assistance, advise and kind encouragement, without which this work would not have been possible. I am also grateful to Dr. J. J. M. Too and Dr. S. Y. Cheng whose guidence and discussions during the course of this study have been very helpful.

I would like to thank Dr. N. Popplewell and Dr. R. B. Pinkney, the members of my advisory committee, who read through my work and gave valuable ideas and comments. Their interest and help are sincerely acknowledged. I am also grateful to the staff members and fellow graduate students at the Mechanical and Civil Engineering Department of the University of Manitoba whose discussions have been very helpful.

I would also like to acknowledge the University of Manitoba Graduate Fellowship Committee, the Department of Mechanical Engineering and my advisor, Dr. T. R. Hsu for the financial supports I have been given during the course of my study here.

TABLE OF CONTENTS

LIST OF FIGURES

NOMENCLATURE

$[A]$	Transformation relating generalized coordinate and nodal displacements
$[B]$	Transformation relating strains and displacements
$\{b\}$	Vector of generalized coordinate
$[C^e],[C^p],[C^{ep}]$	Elastic, plastic and elasto-plastic matrix of material properties respectively
$[D]$	Constitutive stress-strain matrices
E	Young's modulus of elasticity
E'	Plastic modulus
F	General yield function
f^V,f^Z,f^θ	Body force components in a cylindrical coordinate system
G	Shear modulus
$[G]$	Transformation relating strains and generalized coordinate
H'	Slope of the stress--tensorial-strain curve
$[h]$	Transformation relating nodal displacements and generalized coordinate
J_2	Second deviatoric stress invariant
K	Work hardening parameter
$[K],[K]_i^e$	Stiffness matrix of a solid or one of its elements
$[N]$	Shape function, or interpolating function
$\{Q\},\{Q\}_i^e$	Vector of nodal loads of a solid or one of its elements
S,S'	Boundary surface of a solid or one of its elements
T	Transpose of a vector or matrix
t^r,t^Z,t^θ	Surface traction components in a cylindrical coordinate system
$\{u\},\{\varepsilon\},\{\sigma\},\{f\},\{t\}$	Vector of displacements, strains, stresses, body forces and surface tractions respectively

U^x, U^y Horizontal and vertical displacement respectively

$\{u\}^e$ Vector of nodal displacements

u^r, u^z, u^θ Displacement components in a cylindrical coordinate system

V, V' Volume of a solid or one of its elements

X, X^e General functional of a solid or one of its elements

Δ, δ Incremental amount

$\{\phi\}, \{\phi\}^e$ Vector of unknown functions or its nodal values

$[\phi]$ Coefficient matrix for generalized coordinate model

ρ Density of materials

α Coefficient of thermal expansion

ν Poisson ratio

δ_{ij} Kronecker delta

$d\lambda$ Prandtl-Reuss material proportionality factor

$\bar{\varepsilon}, \bar{\sigma}$ Effective strain, effective stress

$\{\varepsilon^o\}$ Vector of initial strains

$\varepsilon^{rr}, \varepsilon^{zz}, \varepsilon^{\theta\theta}, \varepsilon^{rz}, \varepsilon^{r\theta}, \varepsilon^{z\theta}$ Strain components in a cylindrical coordinate system

$\sigma^{rr}, \sigma^{zz}, \sigma^{\theta\theta}, \sigma^{rz}, \sigma^{r\theta}, \sigma^{z\theta}$ Stress components in a cylindrical coordinate system

σ_k Auxiliary stress close to elasto-plastic transition (sigma bi-linear kink)

$\sigma'_{ij}, \{\sigma'\}$ Vector of deviatoric stress components

τ_y, σ_y Experimentally determined yield stress in pure shear and in uniaxial tension test respectively

$\{d\varepsilon\}, \{d\varepsilon^e\}, \{d\varepsilon^p\}$ Vector of incremental strain, incremental elastic strain and incremental plastic strain components

CHAPTER I

INTRODUCTION

1.1 Object of Study

The method of Finite Element Analysis has been widely used in structural engineering and many other engineering fields for almost twenty years [1]. Within the context of structural mechanics, the early work was mostly centered on the elastic analysis of two-dimensional plane problems, plate bending, shells and three-dimensional problems [2]. However, as emphasis has gradually been shifted to ultimate load analysis for efficient design, particullarly in technologically advanced fields such as reactor vessel and aircraft design, the inclusion of non-linear elasto-plastic analysis has become desirable. Several two-dimensional elasto-plastic analysis computer codes and examples have been published and good comparisons with analytical solutions or experimental results have been reported [3 - 7]. In recent years, some three-dimensional elasto-plastic analysis computer codes have also been made available for use wherever the assumption of planar model is invalid [8 - 10].

Many researchers have reported a tremendous increase in the amount of data preparation, computer core storage and computational effort in a three-dimensional finite element analysis [11] over two-dimensional analysis. The increase becomes even more disproportionate for elasto-plastic analyses [8 - 10]. Fortunately,

many complex three-dimensional engineering structures in advanced nuclear and aerospace industries are axisymmetric solids or shells of revolution; nuclear pressure vessels, CANDU reactor fuel elements and rocket nozzles are practical examples of such structures. Structures of this type subjected only to axisymmetric loading can be treated as two-dimensional problems because of the circumferential independence of the solutions. Furthermore, structures of this type subjected to non-axisymmetric loading were also simplified,within the elastic range, by making use of the Fourier expansion method to represent the circumferential dependence of solutions [12, 13]. A substantial saving in data preparation and computational effort can be achieved by using this technique.

To the present, however, the application of this combined finite element and Fourier expansion method has not been reported feasible for the more complicated and interesting area of elasto-plastic analysis. It is the object of this thesis to study the feasibility of applying this method to elasto-plastic analysis, with the anticipation that this study will lead, in the near future, to further development of thermo-mechanically coupled analysis.

1.2 Literature Review

The modern finite element method is generally recognized to have originated with an engineering group led by M.J. Turner at the

Boeing Company to work on aircraft structural dynamics problems [1]. Since then, many significant advances have been made to extend the method for handling structural problems such as plate bending, thin shells, three-dimensional structures and large-deflection and stability problems [15].

It was not until 1960 that the initial inelastic finite element formulations were published [16]. This early work used initial strains in conjunction with the finite element method to account for material non-linearity. Another alternative approach to the inelastic structural problem was reported later, in 1965 [17]. The approach replaces the iterative calculations of the initial-strain approach by a piecewise linear solution, through incremental stress-strain relations.

The period from 1965 onwards may well be known as the golden age of finite element development. Many conference proceedings and summary papers have been made public. Among them are the First Conference on Matrix Methods in Structural Mechanics held by the Air Force Institute of Technology at Wright-Patterson Air Force Base, Dayton, Ohio in 1965 [2], the Second and Third Conferences held in 1968 and 1971 [2, 18] and the First and Second Japan-United States Seminars on Matrix Methods of Structural Analysis and Design held in Tokyo and Berkeley, California in 1969 and 1972 [7, 19].

Within the context of elasto-plastic finite element analysis,

Yamada [20], Zienkiewicz [21] and Marcal and King [22] reported a general formulation of elasto-plastic work-hardening material behavior. The derivation was based on the Von Mises yield criterion and the Prandtl-Reuss incremental stress-strain relationship. More recent advances have gone in the direction of accelerating the analysis procedure by employing different approaches to the problem. Among them are the iterative, initial stress, initial strain and combined methods [4,11,14,23]. Many two-dimensional and three-dimensional computer programs utilizing these methods have been reported in Refs. [3 - 10].

It was around 1965 that the problems of axisymmetric structures attracted attention by analysts. Wilson, Clough and others applied the finite element method not only to the problem of elastic solids of revolution subject to axisymmetric loadings, but also to the case of non-axisymmetric loading by making use of the Fourier expansion method [12,13,24,25]. The combined finite element and Fourier expansion method was later applied to many other engineering problems, such as the " Finite Strip " method for the elastic behavior of plates, box girders, shells and folded plates [26], and the " Finite Prism " method for elastic box-bridges [27]. Other analysts tried to improve accuracy and efficiency by using higher order elements, quadrilaterals and isoparametric elements [28 - 30].

Another attempt has also been made to improve the basic accuracy of different elements for the method. In general this involves the use of approximate integration techniques which disregard part of the shear strain energy associated with pure bending modes, or the presence of the incompatible displacement modes at the elements [6, 30]. However, to the best of the author's knowledge, no attempt has been made to solve elasto-plastic problems by this method.

CHAPTER II

THEORETICAL BACKGROUNDS

2.1 Introduction of The Finite Element Method

Modern finite element theory had its recognizable beginnings in the displacement (or stiffness) method of structure analysis. The initial steps were based on a completely logical extension of the stiffness analysis procedure widely used for bar structures (frames, trusses, etc.) to accommodate surface structures (plates, shells, etc.) and continua (three-dimensional solids including solids or shells of revolution). The structure (two-dimensional or three-dimensional) is divided into a finite number of discrete parts (elements) and these elements are interconnected at their apexes (nodes) to form an idealized structure system as shown in Figure 1. A simple form of displacement pattern applies to each element of the structure system and the virtual work of each element is calculated accordingly. The equilibrium of virtual work of the idealized structure system provides a set of linear algebraic equations called "Stiffness Equation". With the prescribed boundary conditions, the stiffness equation can be solved to find the displacements at each node and the stresses and strains at each element of the idealized structure system [Ref. 14, pp. 16-32].

It was later discovered that this early work could be fully developed from the variational principles of elasticity [Ref. 14, pp. 33-47]. This discovery has widened the applications of the finite element

method to other engineering problems to which the variational technique are prevailed. Typical examples are heat conduction, fluid flow, soil and rock mechanics, and seepage problems. The variational process for these problems is of course more general.

2.2 The Variational Approach of Finite Element Method

The general theory of variational approach is based on the postulation that the correct solution is the one minimizing some quantity X which is defined by suitable integration of the unknown quantities $\{\phi\}$ over the whole domain. Such a integral quantity X is usually known as a "Functional" and may be expressed as [14]:

$$X = \int_V f(\{\phi\}, \frac{\partial}{\partial x}\{\phi\}\ldots)dV + \int_S g(\{\phi\}, \frac{\partial}{\partial x}\{\phi\}\ldots)dS \qquad (2-2-1)$$

where V is the domain of the region, S is part of its boundary which the unknown function, $\{\phi\}$, or its derivatives $\frac{\partial}{\partial x}\{\phi\}$---- etc. exist.

Let the region be divided into discrete elements and be interconnected at nodes as described before. A simple pattern is assumed to correlate the unknown function $\{\phi\}$ with its nodal values $\{\phi\}^e$, or:

$$\{\phi\} = [N]\{\phi\}^e \qquad (2-2-2)$$

where [N] is usually called "Shape function" which is a function of coordinates only.

To minimize the functional X with respect to the total number, M, of the unknown nodal values $\{\phi\}^e$ in the whole domain, a system of

equations:

$$\frac{\partial X}{\partial \{\phi\}^e} = \begin{Bmatrix} \frac{\partial X}{\partial \{\phi\}^e_1} \\ \frac{\partial X}{\partial \{\phi\}^e_2} \\ \vdots \\ \frac{\partial X}{\partial \{\phi\}^e_M} \end{Bmatrix} = 0 \qquad (2-2-3)$$

is provided. Then a typical equation (2-2-3) may be expressed as:

$$\frac{\partial X}{\partial \{\phi\}^e_i} = \Sigma \frac{\partial X^e}{\partial \{\phi\}^e_i} \qquad (2-2-4)$$

where X^e is a typical "sub-functional" of each element.

In a special case where X^e is a quadratic function of $\{\phi\}^e$ and its derivaties, the minimization (2-2-4) becomes:

$$\frac{\partial X^e}{\partial \{\phi\}^e_i} = [K]^e_i \{\phi\}^e_i + \{F\}^e_i = 0 \qquad (2-2-5)$$

in which $[K]^e_i$ and $\{F\}^e_i$ are matrices of constants of a typical element.

Now the minimization of equation (2-2-3) can be simply written as:

$$\frac{\partial X}{\partial \{\phi\}^e} = [K]\{\phi\}^e + \{F\} = 0 \qquad (2-2-6)$$

in which

$$[K] = \Sigma [K]^e_i$$
$$\{F\} = \Sigma \{F\}^e_i \qquad (2-2-7)$$

with summations over all elements. The approach actually yields a set of linear algebraic equations which may be solved by typical computer program.

2.3 Stiffness Equation of Elastic Axisymmetric Solids Subject to Axisymmetric Loadings

In the context of structural mechanics, the "functional", similar to X in equation (2-2-1), can be written as [Ref. 11, pp. 59]:

$$X = \int_V [W\{u\}) - \{u\}^T\{f\}]dV - \int_S \{u\}^T \cdot \{t\}\, dS \qquad (2 - 3 - 1)$$

where $\{u\}$ = displacement vector of the structure system

$\{f\}$ = body forces vector

$\{t\}$ = surface fractions vector

V,S = respective volume and surface of the structure system

T = transpose of a vector quantity

and $W(\{u\})$ = strain energy of the system

$$= 1/2\ \{\varepsilon\}^T \{\sigma\} \qquad (2 - 3 - 2)$$

Similar to equation (2-2-2), a simple pattern is assumed to correlate the unknown displacement vector $\{u\}$ with its nodal values $\{u\}^e$ in an element, or:

$$\{u\} = [N]\ \{u\}^e \qquad (2 - 3 - 3)$$

For simplicity, the constant strain triangular torus element shown in Figure 2 for an axisymmetric structure is adopted to demonstrate the mathematical formulation. Details of derivation may be found in Appendix

I. It also should be noticed that because of the circumferential independence of solution, the assumed displacement pattern includes only the axial and radial coordinates.

The general Hooke's formula including the initial strains * $\{\varepsilon_o\}$:

$$\{\sigma\} = [C^e]\ (\{\varepsilon\} - \{\varepsilon_o\}) \qquad (2-3-4)$$

and the strain-displacement relationship:

$$\{\varepsilon\} = \begin{Bmatrix} \varepsilon_{rr} \\ \varepsilon_{zz} \\ \varepsilon_{\theta\theta} \\ \varepsilon_{rz} \end{Bmatrix} = \begin{Bmatrix} \frac{\partial u_r}{\partial r} \\ \frac{\partial u_z}{\partial z} \\ \frac{u_r}{r} \\ \frac{\partial u_r}{\partial z} + \frac{\partial u_z}{\partial r} \end{Bmatrix} \qquad (2-3-5)$$

in the cylindrical coordinate system simplify the strain energy term as:

$$W(\{u\}) = 1/2\ \{\varepsilon\}^T\ \{\sigma\} \qquad (2-3-6)$$

$$= 1/2\ \{\varepsilon\}^T [C^e](\{\varepsilon\} - \{\varepsilon_o\})$$

$$= \{u\}^e\ (1/2[B]^T[C^e][B]\{u\}^e - [B]^T[C^e]\{\varepsilon_o\})$$

in which [B] is a matrix of coordinates obtained by operating equation (2-3-5) on equation (2-3-3) and $[C^e]$ is the material property matrix relating stresses and strains during elastic deformation.

* initial strains are usually due to temperature change, shrinkage, crystal growth, etc.

In analogy with equation (2-3-1), the " sub-functional ", X^e, of a typical element can be expressed as :

$$X^e = \{u\}^e \int_V (1/2[B]^T[C^e][B]\{u\}^e - [B]^T[C^e]\{\varepsilon_o\} - [N]^T\{f\})dV$$

$$- \{u\}^e \int_S [N]^T\{t\}\, dS \qquad (2-3-7)$$

Minimization of X^e with respect to u^e for a typical element yields the stiffness equation :

$$[K]_i^e\{u\}_i^e = \{Q\}_i^e \qquad (2-3-8)$$

in which

$$[K]_i^e = \int_{V'} [B]^T[C^e][B]dV' \qquad (2-3-9)$$

$$\{Q\}_i^e = \int_{V'} [N]\{f\}dV' + \int_{S'} [N]\{t\}dS' + \int_{V'} [B]^T[C^e]\{\varepsilon_o\}dV' \qquad (2-3-10)$$

and v',s' are the respective volume and surface of a typical torus triangular element.

The total stiffness equation of the system

$$[K]\ \{u\}^e = \{Q\} \qquad (2-3-11)$$

may be assembled in the same way as that in equation (2-2-7).

2.4 Elasto-plastic Analysis of Axisymmetric Solids subject to Axisymmetric Loadings

Considerable amount of theories and computer codes in the area of elasto-plastic analysis has been reported in the past [2 to 11]

[23]. Among them the incremental strain methods are commonly used. The detail derivations of the method may be found in research reports such as those by Ueda [31], Yamada [32], Gallagher [33] and Hsu [34]. This method is basically a step-wise linear incremental analysis to simulate the elasto-plastic material behavior. If the existence of incremental stationarity of the functional (or potential energy in the case of structural mechanics) similar to that of equation (2-2-6) is postulated, the incremental stiffness equation of the structure system:

$$[K]_\ell \{\Delta u\}_\ell = \{\Delta Q\}_\ell \qquad (2-4-1)$$

may be obtained in a more or less straightforward manner. $\{\Delta Q\}_\ell$ and $\{\Delta u\}_\ell$ in Equation (2-4-1) represent respectively the incremental load vector and the incremental displacement vector in a typical loading step ℓ.

Thus, for elastic situation the procedure is nothing but a stepwise summation of the incremental elastic strains $\{\delta\varepsilon^e\}$ calculated in each incremental loading step. Further, when the process reaches the situation that the stress level of one or some of the element is above the yielding point, plastic material behavior should be taken into account in the formulation of incremental stiffness equation (2-4-1). The total strain at this step should include the plastic component $\{\delta\varepsilon^p\}$ or:

$$\{\delta\varepsilon\} = \{\delta\varepsilon^e\} + \{\delta\varepsilon^p\} \qquad (2-4-2)$$

To complete the analysis, it is necessary to have: (i) a yield criterion to acertain the state of stresses at which yielding

is considered to begin, (ii) a flow rule to explain the post-yielding behavior of the material, (iii) a hardening rule obtained from the elasto-plastic stress-strain relationship derived from material test. These three requirements are described respectively in the following:

(i) Yielding criterion:

Of several proposed yield critera, namely,the Tresca, Coulomb, and Von Mises criteria [35], the latter usually fits the experimental data better and is considered to be the most practical and reliable criterion. It states that yield of materials is caused by the maximum distortion energy. For an isotropic material, the yielding surface may be expressed as:

$$F = J_2 - \tau_y^2 = J_2 - \frac{1}{3}\sigma_y^2 = 0 \qquad (2-4-3)$$

in which J_2 = second deviatoric stress invariant

$= 1/2\ \sigma_{ij}'\ \sigma_{ij}'$

σ_{ij}' = deviatoric stress components

$= \sigma_{ij} - \sigma_m$ ($i,j = r,z,\theta$ in cylindrical coordinate system)

$\sigma_m = 1/3\ \delta_{ij}\ \sigma_{ij}$

δ_{ij} = Kronecker delta $= \begin{cases} 0 & (i \neq j) \\ 1 & (i = j) \end{cases}$

and τ_y, σ_y = experimentally determined yield stress in pure shear and in uniaxial tension test respectively.

This criterion further implies that if the state of stress is such that $F < 0$, the material is in the elastic region, that is, $\{\delta\varepsilon^p\} = 0$, and that if $F = 0$, a plastic state is attained and plastic behavior has to be taken into account. No significance is attached to the case $F > 0$.

(ii) Flow Rule:

Generally, there are two major theories that describe the plastic behavior of materials: the deformation (or Hencky) theory and the incremental or flow theory [11]. The former assumes that the total plastic strain components are related to the current stress and are independent of loading path, while the latter assumes that the incremental plastic strain components are a function of the current stress, the strain increments, and the stress increments, i.e :

$$\{d\varepsilon^p\} = \{d\varepsilon^p\}\ (\{\sigma\}, \{d\varepsilon\}, \{d\sigma\}, K) \qquad (2-4-4)$$

where "d" denotes an increment and K is the hardening parameter. Since the plastic strain can not in general be independent of the loading path, the flow theory is considered more practical in applications.

Now, considering equation (2-4-2) in the incremental form, or:

$$\{d\varepsilon\} = \{d\varepsilon^e\} + \{d\varepsilon^p\} \quad * \qquad (2-4-5)$$

in which:

$$\{d\varepsilon\} = [D]\{d\sigma\} = [C^e]^{-1}\{d\sigma\} \qquad (2-4-6)$$

The last two equations can be combined to give:

$$\{d\sigma\} = [C^e]\ (\{d\varepsilon\} - \{d\varepsilon^p\}) \qquad (2-4-7)$$

which may be written as:

$$\{d\sigma\} = [C^{ep}]\ \{d\varepsilon\} \qquad (2-4-8)$$

where $[C^{ep}]$ is called the elasto-plastic matrix and is expressed as:

$$[C^{ep}] = [C^e] - [C^p] \qquad (2-4-9)$$

---

* for convenience, strain components in elasto-plastic analysis are in tensorial form, i.e. $\varepsilon_{ij} = \frac{1}{2}\left(\frac{\partial u_i}{\partial x_j} - \frac{\partial u_j}{\partial x_i}\right)$, rather than the engineering form in elastic analysis.

To obtain the elasto-plastic matrix $[C^{ep}]$, two sets of information are needed: the slope (H') of the tangent to the effective stress-effective plastic strain ($\bar{\sigma}$ - $\bar{\varepsilon}^p$) diagram, otherwise known as the hardening coefficient, and the "flow rule", or description of the differential changes in the plastic strain component $\{d\varepsilon^p\}$ as expressed in equation (2-4-4).

With respect to H', it is apparent from Figure 3 that:

$$H' \, d\bar{\varepsilon}^p = d\bar{\sigma} \qquad (2-4-10)$$

in which effective stress $\bar{\sigma}$ and effective plastic strain increment $d\bar{\varepsilon}^p$ are defined as:

$$\bar{\sigma} = \left(\frac{3}{2}\, \sigma_{ij}' \, \sigma_{ij}'\right)^{1/2} \qquad (2-4-11)$$

$$= \frac{1}{\sqrt{2}} \left[(\sigma_{\gamma\gamma}-\sigma_{zz})^2 + (\sigma_{zz}-\sigma_{\theta\theta})^2 + (\sigma_{\theta\theta}-\sigma_{\gamma\gamma})^2 + 6(\sigma_{rz}^2 + \sigma_{r\theta}^2 + \sigma_{z\theta}^2)\right]^{1/2}$$

$$d\bar{\varepsilon}^p = \frac{\sqrt{2}}{3} \left[(d\varepsilon_{\gamma\gamma}^p - d\varepsilon_{zz}^p)^2 + (d\varepsilon_{zz}^p - d\varepsilon_{\theta\theta}^p)^2 + (d\varepsilon_{\theta\theta}^p - d\varepsilon_{\gamma\gamma}^p)^2 + 6(d\varepsilon_{\gamma z}^{p\,2} + d\varepsilon_{z\theta}^{p\,2} + d\varepsilon_{\gamma\theta}^{p\,2})\right]^{1/2}$$

$$(2-4-12)$$

For the flow rule, the Prandtl-Reuss representation with isotropic hardening states that the plastic strain component increments are proportional to the deviatoric stress components (σ')[32], or:

$$\{d\varepsilon^p\} = \{\sigma'\}\, d\lambda \qquad (2-4-13)$$

in which $d\lambda$ = proportionality factor.

(iii) Hardening rule:

The general yield criterion which takes only the state

of stress $\{\sigma\}$ and "hardening" parameter K* into account, is

$$F(\{\sigma\}, K) = 0 \qquad (2-4-14)$$

and its differential form is :

$$dF = \{\frac{\partial F}{\partial \sigma}\}^T \{d\sigma\} + \frac{\partial F}{\partial K} dK \qquad (2-4-15)$$

or, expressing the hardening in terms of plastic strains ,

$$dF = \{\frac{\partial F}{\partial \sigma}\}^T \{d\sigma\} + \frac{\partial F}{\partial K} \{\frac{\partial K}{\partial \varepsilon^P}\}\{d\varepsilon^P\} \qquad (2-4-17)$$

Substituting equation (2-4-7), (2-4-13) into equation (2-4-17), one obtains:

$$\{\frac{\partial F}{\partial \sigma}\}^T [C^e](\{d\varepsilon\} - \{\sigma'\}d\lambda) + \frac{\partial F}{\partial K} \{\frac{\partial K}{\partial \varepsilon^P}\}^T \{\sigma'\}d\lambda = 0 \qquad (2-4-18)$$

Solving for $d\lambda$ using equation (2-4-18), the following is obtained:

$$d\lambda = \frac{\{\frac{\partial F}{\partial \sigma}\}^T [C^e] \{d\varepsilon\}}{\{\frac{\partial F}{\partial \sigma}\}^T [C^e]\{\sigma'\} - \frac{\partial F}{\partial K} \{\frac{\partial K}{\partial \varepsilon^P}\}^T \{\sigma'\}} \qquad (2-4-19)$$

Substituting $d\lambda$ into equation (2-4-13), one obtains :

$$\{d\varepsilon^P\} = \{\sigma'\}\, d\lambda = \frac{\{\sigma'\}\{\frac{\partial F}{\partial \sigma}\}^T [C^e]}{S} \{d\varepsilon\} \qquad (2-4-20)$$

in which:
$$S = \{\frac{\partial F}{\partial \sigma}\}^T [C^e]\{\sigma'\} - \frac{\partial F}{\partial K} \{\frac{\partial K}{\partial \varepsilon^P}\}^T \{\sigma'\} \qquad (2-4-21)$$

---

* [Ref. 14, pp. 380] "work hardening" material is represented by the amount of plastic work done during the plastic deformation, or:

$$dK = \{\sigma\}^T \{d\varepsilon^P\} \qquad (2-4-16)$$

Comparison between equation (2-4-20) and equation (2-4-7) yields:

$$[C^p] = \frac{[C^e]\{\sigma'\}\{\frac{\partial F}{\partial \sigma}\}^T [C^e]}{S} \qquad (2-4-22)$$

The elasto-plastic matrix $[C^{ep}]$ can now be expressed as:

$$[C^{ep}] = [C^e] - [C^p]$$

$$= [C^e] - \frac{[C^e]\{\sigma'\}\{\frac{\partial F}{\partial \sigma}\}[C^e]}{S} \qquad (2-4-23)$$

Using definitions of F and K as shown in Equation (2-4-3) and Equation (2-4-16), the following can be obtained [21]:

$$\{\frac{\partial F}{\partial \sigma}\} = < \sigma_r', \sigma_z', \sigma_\theta', 2\sigma_{rz}', 2\sigma_{r\theta}', 2\sigma_{z\theta}' >$$

$$\frac{\partial F}{\partial K} = -\frac{2}{3} H'$$

$$\{\frac{\partial K}{\partial \varepsilon^p}\}^T = \{\sigma\}^T \qquad (2-4-24)$$

The elasticity matrix of the stress--tensorial-strain relationship $[C^e]$ is :

$$[C^e] = 2G \begin{bmatrix} \frac{1-\nu}{1-2\nu} & & & & & \\ \frac{\nu}{1-2\nu} & \frac{1-\nu}{1-2\nu} & & & \text{SYM.} & \\ \frac{\nu}{1-2\nu} & \frac{\nu}{1-2\nu} & \frac{1-\nu}{1-2\nu} & & & \\ 0 & 0 & 0 & 1 & & \\ 0 & 0 & 0 & 0 & 1 & \\ 0 & 0 & 0 & 0 & 0 & 1 \end{bmatrix} \qquad (2-4-25)$$

Substitute Equation (2-4-24), (2-4-25) into Equation (2-4-21), (2-4-22), the following may be obtained:

$$S = \frac{4}{9}(3G + H')\,\bar{\sigma}^2 \qquad (2-4-26)$$

and

$$[C^e]\{\sigma'\}\left\{\frac{\partial F}{\partial \sigma}\right\}^T[C^e] = 4G^2$$

$$\times \begin{bmatrix} \sigma_{rr}'^2 & & & & & \\ \sigma_{rr}'\sigma_{zz}' & \sigma_{zz}'^2 & & \text{SYM.} & & \\ \sigma_{rr}'\sigma_{\theta\theta}' & \sigma_{zz}'\sigma_{\theta\theta}' & \sigma_{\theta\theta}'^2 & & & \\ \sigma_{rr}'\sigma_{z\theta}' & \sigma_{zz}'\sigma_{z\theta}' & \sigma_{\theta\theta}'\sigma_{z\theta}' & \sigma_{z\theta}'^2 & & \\ \sigma_{rr}'\sigma_{\theta r}' & \sigma_{zz}'\sigma_{\theta r}' & \sigma_{\theta\theta}'\sigma_{\theta r}' & \sigma_{z\theta}'\sigma_{\theta r}' & \sigma_{\theta r}'^2 & \\ \sigma_{rr}'\sigma_{rz}' & \sigma_{zz}'\sigma_{rz}' & \sigma_{\theta\theta}'\sigma_{rz}' & \sigma_{z\theta}'\sigma_{rz}' & \sigma_{\theta r}'\sigma_{rz}' & \sigma_{rz}'^2 \end{bmatrix} \qquad (2-4-27)$$

$$= 4G^2\,[\text{▨}]$$

where [▨] is the symmetric deviatoric stress matrix given in Equation (2 - 4 - 27).

Accordingly, $[C_p]$ can be obtained as:

$$[C_p] = \frac{2G \cdot \frac{9G}{2\bar{\sigma}^2}\,[\text{▨}]}{3G + H'} = \frac{2G}{S_o}\,[\text{▨}] \qquad (2-4-28)$$

with $$S_o = \frac{2}{3}\bar{\sigma}^2 \left(1 + \frac{H'}{3G}\right) \qquad (2-4-29)$$

The elasto-plastic matrix $[C^{ep}]$ is now in a form with parameters of material properties $[C^e]$, H' and state of stress $\bar{\sigma}$, $\{\sigma'\}$ only, or:

$$[C^{ep}] = 2G \begin{bmatrix} \frac{1-\nu}{1-2\nu} - \frac{\sigma'^2_{rr}}{S_o} & & & & & \\ \frac{\nu}{1-2\nu} - \frac{\sigma'_{rr}\sigma'_{zz}}{S_o} & \frac{1-\nu}{1-2\nu} - \frac{\sigma'^2_{zz}}{S_o} & & & \text{SYM.} & \\ \frac{\nu}{1-2\nu} - \frac{\sigma'_{rr}\sigma'_{\theta\theta}}{S_o} & \frac{\nu}{1-2\nu} - \frac{\sigma'_{zz}\sigma'_{\theta\theta}}{S_o} & \frac{1-\nu}{1-2\nu} - \frac{\sigma'^2_{\theta\theta}}{S_o} & & & \\ -\frac{\sigma'_{rr}\sigma'_{z\theta}}{S_o} & -\frac{\sigma'_{zz}\sigma'_{z\theta}}{S_o} & -\frac{\sigma'_{\theta\theta}\sigma'_{z\theta}}{S_o} & \frac{1}{2} - \frac{\sigma'^2_{z\theta}}{S_o} & & \\ -\frac{\sigma'_{rr}\sigma'_{\theta r}}{S_o} & -\frac{\sigma'_{zz}\sigma'_{\theta r}}{S_o} & -\frac{\sigma'_{\theta\theta}\sigma'_{\theta r}}{S_o} & -\frac{\sigma'_{z\theta}\sigma'_{\theta r}}{S_o} & \frac{1}{2} - \frac{\sigma'^2_{\theta r}}{S_o} & \\ -\frac{\sigma'_{rr}\sigma'_{rz}}{S_o} & -\frac{\sigma'_{zz}\sigma'_{rz}}{S_o} & -\frac{\sigma'_{\theta\theta}\sigma'_{rz}}{S_o} & -\frac{\sigma'_{z\theta}\sigma'_{rz}}{S_o} & -\frac{\sigma'_{\theta r}\sigma'_{rz}}{S_o} & \frac{1}{2} - \frac{\sigma'^2_{rz}}{S_o} \end{bmatrix}$$

$$(2-4-30)$$

In this analysis, experimentally determined elasto-plastic constitutive relations of $\bar{\sigma}$ and $\bar{\varepsilon}$ are approximated by a generalized family of continuous functions [36]:

$$\bar{\sigma} = \frac{E\bar{\varepsilon}}{\left\{1 + \left[\frac{E\bar{\varepsilon}}{(1-\frac{E'}{E})\bar{\sigma}_k + E'\bar{\varepsilon}}\right]^n\right\}^{1/n}} \qquad (2-4-31)$$

where σ_k = auxiliary stress close to elasto-plastic transition (as shown in Fig. 4).

n = a factor which determines abruptness of the transition

E' = limiting value of the slope of the experimentally determined effective stress, $\bar{\sigma}$ effective strain, $\bar{\varepsilon}$ curve.

The value H',which was defined in Eq. (2-4-10) as:

$$H' = \frac{d\bar{\sigma}}{d\bar{\varepsilon}^{P}}$$

may be approximated by:*

$$\begin{aligned} H' &= \frac{1}{\partial\bar{\varepsilon}^{P}/\partial\bar{\sigma}} \\ &\doteq \frac{1}{\frac{\partial\bar{\varepsilon}}{\partial\bar{\sigma}} - \frac{\partial\bar{\varepsilon}^{e}}{\partial\bar{\sigma}}} \\ &\doteq \frac{1}{\frac{1}{E_t} - \frac{1}{E}} \end{aligned} \qquad (2 - 4 - 32)$$

in which

$$E_t = \frac{d\bar{\sigma}}{d\varepsilon} = \frac{E\{1+[\frac{E\bar{\varepsilon}}{(1-\frac{E'}{E})\bar{\sigma}_k + E'\bar{\varepsilon}}]^{n+1}\frac{E'}{E}\}}{\{1+[\frac{E\bar{\varepsilon}}{(1-\frac{E'}{E})\bar{\sigma}_k + E'\bar{\varepsilon}}]^{n}\}^{\frac{n+1}{n}}} \qquad (2 - 4 - 33)$$

according to Equation (2 - 4 - 31).

---

* The approximation of $d\bar{\varepsilon}^{p} = d\bar{\varepsilon} - d\bar{\varepsilon}^{e}$ is valid in the elastic or plastic region and is valid in the elasto-plastic region only if the incremental strain components are reasonably small.

CHAPTER III

ELASTIC ANALYSIS OF AXISYMMETRIC STRUCTURES SUBJECT TO NON-AXISYMMETRIC LOADINGS

3.1 Introduction

The technique of solving problems of solids of revolution or shells subject to axisymmetric loadings has been demonstrated in Chapter II. It happens, however, that in many situations,structures of this kind are subjected to non-axisymmetric loadings. Typical examples are cylindrical pressure vessels horizontally mounted, large pipelines, CANDU type nuclear fuel elements, etc.;all fall into this category. Wilson and others [12, 13] have reported that combined finite element and Fourier expansion method is capable of handling this kind of problem within the elastic limit. This method is not limited to structural problems in the general sense. The variational approach described below is applicable to other engineering problems, for which the finite element method can be used.

3.2 Stiffness Equation of Elastic Axisymmetric Solids Subject to Non-axisymmetric Loadings

Consider first an axisymmetric solid as shown in Figure 5. The solid is subjected to non-axisymmetric loading components {f} (body forces) and {t} (surface tractions) which may be expanded in a Fourier

series as:

$$\{f\} = \begin{Bmatrix} f^r \\ f^z \\ f^\theta \end{Bmatrix}_{(r,z,\theta)} = \sum_n \begin{Bmatrix} f^r_n\,(r,z) \cdot \cos n\theta \\ f^z_n\,(r,z) \cdot \cos n\theta \\ f^\theta_n\,(r,z) \cdot \sin n\theta \end{Bmatrix} \qquad (3-2-1)$$

$$\{t\} = \begin{Bmatrix} t^r \\ t^z \\ t^\theta \end{Bmatrix}_{(r,z,\theta)} = \sum_n \begin{Bmatrix} t^r_n\,(r,z) \cdot \cos n\theta \\ t^z_n\,(r,z) \cdot \cos n\theta \\ t^\theta_n\,(r,z) \cdot \sin n\theta \end{Bmatrix}$$

Because of this non-axisymmetric loading situation, the displacement solution to this problem is obviously no longer independent of the circumferential coordinate (θ), and the circumferential displacement (u^θ) associated with angular direction θ must be considered in the general case. The displacement components are thus assumed to be:

$$\{u\}_{(r,z,\theta)} = \begin{Bmatrix} u^r \\ u^z \\ u^\theta \end{Bmatrix}_{(r,z,\theta)} = \sum_n \begin{Bmatrix} u^r_n\,(r,z) \cdot \cos n\theta \\ u^z_n\,(r,z) \cdot \cos n\theta \\ u^\theta_n\,(r,z) \cdot \sin n\theta \end{Bmatrix}$$

$$(3-2-2)$$

Accordingly, the strain-displacement relationship has to include terms associated with the circumferential components, or:

$$\{\varepsilon\} = \begin{Bmatrix} \varepsilon^{rr} \\ \varepsilon^{zz} \\ \varepsilon^{\theta\theta} \\ \varepsilon^{rz} \\ \varepsilon^{r\theta} \\ \varepsilon^{z\theta} \end{Bmatrix} = \begin{Bmatrix} \frac{\partial u^r}{\partial r} \\ \frac{\partial u^z}{\partial z} \\ \frac{1}{r}\left(\frac{\partial u^\theta}{\partial \theta}\right) + \frac{u^r}{r} \\ \frac{\partial u^r}{\partial z} + \frac{\partial u^z}{\partial r} \\ \frac{1}{r}\left(\frac{\partial u^r}{\partial \theta}\right) + \frac{\partial u^\theta}{\partial r} - \frac{u^\theta}{r} \\ \frac{\partial u^\theta}{\partial z} + \frac{1}{r}\left(\frac{\partial u^z}{\partial \theta}\right) \end{Bmatrix} \qquad (3-2-3)$$

Substitution of Eq. (3-2-2) into the above equations yields:

$$\{\varepsilon\} = \sum_n \begin{Bmatrix} \left(\frac{\partial u_n^r}{\partial z}\right) \cdot \cos n\theta \\ \left(\frac{\partial u_n^z}{\partial z}\right) \cdot \cos n\theta \\ \left(\frac{1}{r}\left(\frac{\partial u_n^\theta}{\partial \theta}\right) + \frac{u_n^r}{r}\right) \cdot \cos n\theta \\ \left(\frac{\partial u_n^r}{\partial z} + \frac{\partial u_n^z}{\partial r}\right) \cdot \cos n\theta \\ \left(\frac{1}{r}\left(\frac{\partial u_n^r}{\partial \theta}\right) + \frac{\partial u_n^\theta}{\partial r} - \frac{u_n^\theta}{r}\right) \cdot \sin n\theta \\ \left(\frac{\partial u_n^\theta}{\partial z} + \frac{1}{r}\left(\frac{\partial u_n^z}{\partial \theta}\right)\right) \cdot \sin n\theta \end{Bmatrix}$$

or

$$\{\varepsilon\} = \sum_n \begin{Bmatrix} \varepsilon_n^{rr}(r,z) \cdot \cos n\theta \\ \varepsilon_n^{zz}(r,z) \cdot \cos n\theta \\ \varepsilon_n^{\theta\theta}(r,z) \cdot \cos n\theta \\ \varepsilon_n^{rz}(r,z) \cdot \cos n\theta \\ \varepsilon_n^{r\theta}(r,z) \cdot \sin n\theta \\ \varepsilon_n^{z\theta}(r,z) \cdot \sin n\theta \end{Bmatrix} \qquad (3-2-4)$$

in which

$$\begin{Bmatrix} \varepsilon_n^{rr} \\ \varepsilon_n^{zz} \\ \varepsilon_n^{\theta\theta} \\ \varepsilon_n^{rz} \\ \varepsilon_n^{r\theta} \\ \varepsilon_n^{z\theta} \end{Bmatrix}_{(r,z)} = \{\varepsilon_n\} = \begin{Bmatrix} \frac{\partial u_n^r}{\partial r} \\ \frac{\partial u_n^z}{\partial z} \\ \frac{1}{r}\left(\frac{\partial u_n^\theta}{\partial \theta}\right) + \frac{u_n^r}{r} \\ \frac{\partial u_n^r}{\partial z} + \frac{\partial u_n^z}{\partial r} \\ \frac{1}{r}\left(\frac{\partial u_n^r}{\partial \theta}\right) + \frac{\partial u_n^\theta}{\partial r} - \frac{u_n^\theta}{r} \\ \frac{\partial u_n^\theta}{\partial z} + \frac{1}{r}\left(\frac{\partial u_n^z}{\partial \theta}\right) \end{Bmatrix} \qquad (3-2-5)$$

Within the elastic range, stress components are related to strain components by :

$$\{\sigma\} = [C^e]\{\varepsilon\}$$

or

$$\{\sigma\} = \sum_n [C^e] \begin{Bmatrix} \varepsilon_n^{rr} \cdot \cos n\theta \\ \varepsilon_n^{zz} \cdot \cos n\theta \\ \varepsilon_n^{\theta\theta} \cdot \cos n\theta \\ \varepsilon_n^{rz} \cdot \cos n\theta \\ \varepsilon_n^{r\theta} \cdot \sin n\theta \\ \varepsilon_n^{z\theta} \cdot \sin n\theta \end{Bmatrix} \qquad (3-2-6)$$

in which the stress components can be expressed as:

$$\{\sigma\} = \sum_n \begin{Bmatrix} \sigma_n^{rr}(r,z) \cdot \cos n\theta \\ \sigma_n^{zz}(r,z) \cdot \cos n\theta \\ \sigma_n^{\theta\theta}(r,z) \cdot \cos n\theta \\ \sigma_n^{rz}(r,z) \cdot \cos n\theta \\ \sigma_n^{r\theta}(r,z) \cdot \sin n\theta \\ \sigma_n^{z\theta}(r,z) \cdot \sin n\theta \end{Bmatrix} \qquad (3-2-7)$$

with $\{\sigma_n\} = [C^e]\{\varepsilon_n\}$.

Now, consider the functional of the elasticity problem for a typical torus element as that shown in Eq. (2-3-1), or:

$$X^e = \int_{V'} \left(\frac{1}{2}\{\varepsilon\}^T\{\sigma\} - \{u\}^T\{f\}\right) dV' - \int_{S'} \{u\}^T\{t\}\, dS' \qquad (3-2-8)$$

in which V', S' are the respective volume and boundary surfaces of the element and dV', dS' may be expressed as (r dr dz dθ),(dℓ dθ) as shown in Appendix I.

Substitute Eq. (3-2-1), (3-2-2), (3-2-4) and (3-2-6) into Eq. (3-2-8), one obtains:

$$X^e = \int_r\int_z\int_o^{2\pi}\left(\left(\frac{1}{2}\sum_m \begin{Bmatrix} \varepsilon_m^{rr}\cdot\cos m\theta \\ \varepsilon_m^{zz}\cdot\cos m\theta \\ \varepsilon_m^{\theta\theta}\cdot\cos m\theta \\ \varepsilon_m^{rz}\cdot\cos m\theta \\ \varepsilon_m^{r\theta}\cdot\sin m\theta \\ \varepsilon_m^{z\theta}\cdot\sin m\theta \end{Bmatrix}^T\right)\cdot\left(\sum_n \begin{Bmatrix} \sigma_n^{rr}\cdot\cos n\theta \\ \sigma_n^{zz}\cdot\cos n\theta \\ \sigma_n^{\theta\theta}\cdot\cos n\theta \\ \sigma_n^{rz}\cdot\cos n\theta \\ \sigma_n^{r\theta}\cdot\sin n\theta \\ \sigma_n^{z\theta}\cdot\sin n\theta \end{Bmatrix}\right) - \left(\sum_m \begin{Bmatrix} u_m^r\cdot\cos m\theta \\ u_m^z\cdot\cos m\theta \\ u_m^\theta\cdot\sin m\theta \end{Bmatrix}^T\right)$$

$$\left(\sum_n \begin{Bmatrix} f_n^r\cdot\cos n\theta \\ f_n^z\cdot\cos n\theta \\ f_n^\theta\cdot\sin n\theta \end{Bmatrix}\right)d\theta\, r dr\, dz - \int_\ell\int_o^{2\pi}\left(\sum_m \begin{Bmatrix} u_m^r\cdot\cos m\theta \\ u_m^z\cdot\cos m\theta \\ u_m^\theta\cdot\sin m\theta \end{Bmatrix}^T\right)\left(\sum_n \begin{Bmatrix} t_n^r\cdot\cos n\theta \\ t_n^z\cdot\cos n\theta \\ t_n^\theta\cdot\sin n\theta \end{Bmatrix}\right)d\theta\, d\ell$$

or:

$$X^e = \int_r\int_z\int_o^{2\pi}\left[\sum_m\sum_n\left(\frac{1}{2}\begin{Bmatrix} \varepsilon_m^{rr}\cdot\cos m\theta \\ \varepsilon_m^{zz}\cdot\cos m\theta \\ \varepsilon_m^{\theta\theta}\cdot\cos m\theta \\ \varepsilon_m^{rz}\cdot\cos m\theta \\ \varepsilon_m^{r\theta}\cdot\sin m\theta \\ \varepsilon_m^{z\theta}\cdot\sin m\theta \end{Bmatrix}^T[C^e]\begin{Bmatrix} \varepsilon_n^{rr}\cdot\cos n\theta \\ \varepsilon_n^{zz}\cdot\cos n\theta \\ \varepsilon_n^{\theta\theta}\cdot\cos n\theta \\ \varepsilon_n^{rz}\cdot\cos n\theta \\ \varepsilon_n^{r\theta}\cdot\sin n\theta \\ \varepsilon_n^{z\theta}\cdot\sin n\theta \end{Bmatrix} - \begin{Bmatrix} u_m^r\cdot\cos m\theta \\ u_m^z\cdot\cos m\theta \\ u_m^\theta\cdot\sin m\theta \end{Bmatrix}^T\begin{Bmatrix} f_n^r\cdot\cos n\theta \\ f_n^z\cdot\cos n\theta \\ f_n^\theta\cdot\sin n\theta \end{Bmatrix}\right)\right]d\theta\, r dr\, dz$$

$$-\int_{\ell}\int_{o}^{2\pi} \left(\sum_{m}\sum_{n} \begin{Bmatrix} u_m^r \cdot \cos m\theta \\ u_m^z \cdot \cos m\theta \\ u_m^\theta \cdot \sin m\theta \end{Bmatrix}^T \begin{Bmatrix} t_n^r \cdot \cos n\theta \\ t_n^z \cdot \cos n\theta \\ t_n^\theta \cdot \sin n\theta \end{Bmatrix}\right) d\theta \, d\ell$$

(3 - 2 - 9)

The following orthogonality relations of trigonometric functions:

$$\int_o^{2\pi} (\cos m\theta)\cdot(\cos n\theta)d\theta = \begin{cases} 2\pi & \text{for } m = n = 0 \\ \pi & m = n \neq 0 \\ 0 & m \neq n \end{cases}$$

$$\int_o^{2\pi} (\sin m\theta)\cdot(\sin n\theta)d\theta = \begin{cases} \pi & \text{for } m = n \neq 0 \\ 0 & m \neq n \text{ and } m = n = 0 \end{cases}$$

and

$$\int_o^{2\pi} (\cos m\theta)\cdot(\sin n\theta)d\theta = 0 \quad \text{for all } m \text{ and } n$$

may be used to simplify X^e as:

$$X^e = \eta \left(\sum_n \int_r\int_z \left(\frac{1}{2}\{\varepsilon_n\}^T[C^e]\{\varepsilon_n\} - \{u_n\}^T\{f_n\}\right)rdrdz - \int_\ell \{u_n\}^T\{t_n\}d\ell\right)$$

$$= \eta \sum_n X_n^e \qquad \text{(3 - 2 - 11)}$$

in which

$$\eta = \begin{cases} 2\pi & \text{for } n = 0 \\ \pi & n \neq 0 \end{cases}$$

and

$$X_n^e = \int_r\int_z \left(\frac{1}{2}\{\varepsilon_n\}^T[C^e]\{\varepsilon_n\} - \{u_n\}^T\{f_n\}\right)rdrdz - \int_\ell \{u_n\}^T\{t_n\}d\ell$$

(3 - 2 - 12)

It should be noted that this simplification is possible only for the case that $\{\varepsilon_m\}$, $\{u_n\}$, $\{f_n\}$, $\{t_n\}$ and $[C^e]$ are circumferential-coordinate-independent.

Equation (3-3-11) shows that functional X^e is actually the sum of N sub-functional X_n^e. Similar to Eq. (2-2-5), minimization of each sub-functional X_n^e with respect to $\{u_n\}^e$ yields N set of stiffness equations, or:

$$[K_n]\{u_n\}^e = \{F_n\} \qquad n = 1, 2, \ldots N \qquad (3 - 3 - 13)$$

and each stiffness equation (2-3-13) may be solved to obtain the displacement solution of each individual mode n. The exact solution of the displacement components $\{u\}^e$, or stress components $\{\sigma\}$ may be summed up for all modes according to Eq. (3-2-2) or (3-2-6) respectively. Detailed formulation of the stiffness equation for a triangular torus element is given in Appendix II.

3.3 Computer Code and Sample Problem

A rather simple program code called "NLSTRS", which includes only constant strain triangular and quadrilateral elements was developed by the author to demonstrate the validity of this combined finite element and Fourier expansion method. It is based on another code called "ELSTRS", which is capable of handling plane problems, axisymmetric structures under axisymmetric loadings only.

The sample problem of a heavy beam with circular cross-section bent by its own weight is chosen to test the validity of the "NLSTRS"

code. Reasons for choosing this sample problem are simply that the loading situation includes only mode 1 body force and that the analytical solution of the problem derived from theory of linear elasticity is available. Computer results of the sample problem showed good comparison with the analytical solutions given by Pearson's exact beam theory [37]. A detailed description of the sample problem and solutions may be found in Appendix III.

CHAPTER IV

ELASTO-PLASTIC ANALYSIS OF AXISYMMETRIC STRUCTURES SUBJECT TO NON-AXISYMMETRIC LOADINGS

4.1 Introduction

The technique of combined finite element and Fourier expansion method for describing the elastic behaviour of axisymmetric solids subject to non-axisymmetric loadings has been demonstrated in Chapter III. Solutions of three-dimensional nature* of this type of problems can be obtained with the computational efforts comparable to those required for plane problems. In this chapter, the feasibility of using this method for the non-linear elasto-plastic analysis will be described.

To begin the analysis, the assumption of the existence of incremental stationarity of a functional (or potential energy) such as postulated in Chapter II has to be maintained, or :

$$\chi^e = \int_{V'} [1/2\{\Delta\varepsilon\}^T\{\Delta\sigma\} - \{\Delta u\}^T\{\Delta f\}]\, dV' - \int_{S'} \{\Delta u\}^T\{\Delta t\}\, dS' \qquad (4-1-1)$$

and $$\frac{\partial F}{\partial \{\Delta u\}} = 0$$

in which $\{\Delta u\}$, $\{\Delta\varepsilon\}$, $\{\Delta\sigma\}$,$\{\Delta f\}$ and $\{\Delta t\}$ are the respective

---

* Solutions that include three independent displacement components, six independent stresses and strains components, i.e. u^r, u^z, u^θ and σ^{rr} ,σ^{zz} ,$\sigma^{\theta\theta}$,σ^{rz} ,$\sigma^{r\theta}$,$\sigma^{z\theta}$,ε^{rr} ,ε^{zz} ,....etc. in a cylindrical coordinate system.

incremental displacement, strain, stress, body force and surface traction components.

Similar to Eq. (3-2-1) and (3-2-2) in Chapter III, the incremental body force , surface traction and displacement components are also assumed to be represented by a Fourier series, or :

$$\{\Delta f\} = \begin{Bmatrix} \Delta f^r \\ \Delta f^z \\ \Delta f^\theta \end{Bmatrix}_{(r,z,\theta)} = \sum_n \begin{Bmatrix} \Delta f^r_{n(r,z)} \cdot \cos n\theta \\ \Delta f^z_{n(r,z)} \cdot \cos n\theta \\ \Delta f^\theta_{n(r,z)} \cdot \sin n\theta \end{Bmatrix} \qquad (4\text{-}1\text{-}2)$$

$$\{\Delta t\} = \begin{Bmatrix} \Delta t^r \\ \Delta t^z \\ \Delta t^\theta \end{Bmatrix}_{(r,z,\theta)} = \sum_n \begin{Bmatrix} \Delta t^r_{n(r,z)} \cdot \cos n\theta \\ \Delta t^z_{n(r,z)} \cdot \cos n\theta \\ \Delta t^\theta_{n(r,z)} \cdot \sin n\theta \end{Bmatrix} \qquad (4\text{-}1\text{-}3)$$

and

$$\{\Delta u\} = \begin{Bmatrix} \Delta u^r \\ \Delta u^z \\ \Delta u^\theta \end{Bmatrix}_{(r,z,\theta)} = \sum_n \begin{Bmatrix} \Delta u^r_{n(r,z)} \cdot \cos n\theta \\ \Delta u^z_{n(r,z)} \cdot \cos n\theta \\ \Delta u^\theta_{n(r,z)} \cdot \sin n\theta \end{Bmatrix} \qquad (4\text{-}1\text{-}4)$$

Accordingly, the strain-displacement relationship similar to that of Eq. (3-2-3), (3-2-4) and (3-2-5) in incremental form may be expressed as :

$$\{\Delta\epsilon\} = \begin{Bmatrix} \Delta\epsilon^{rr} \\ \Delta\epsilon^{zz} \\ \Delta\epsilon^{\theta\theta} \\ \Delta\epsilon^{rz} \\ \Delta\epsilon^{r\theta} \\ \Delta\epsilon^{z\theta} \end{Bmatrix} = \sum_n \begin{Bmatrix} \Delta\epsilon_n^{rr} \cdot \cos n\theta \\ \Delta\epsilon_n^{zz} \cdot \cos n\theta \\ \Delta\epsilon_n^{\theta\theta} \cdot \cos n\theta \\ \Delta\epsilon_n^{rz} \cdot \cos n\theta \\ \Delta\epsilon_n^{r\theta} \cdot \sin n\theta \\ \Delta\epsilon_n^{ze} \cdot \sin n\theta \end{Bmatrix} \qquad (4\text{-}1\text{-}5)$$

$$\{\Delta\epsilon_n\} = \begin{Bmatrix} \Delta\epsilon_n^{rr} \\ \Delta\epsilon_n^{zz} \\ \Delta\epsilon_n^{\theta\theta} \\ \Delta\epsilon_n^{rz} \\ \Delta\epsilon_n^{r\theta} \\ \Delta\epsilon_n^{z\theta} \end{Bmatrix} = \begin{Bmatrix} \dfrac{\partial(\Delta u_n^r)}{\partial r} \\ \dfrac{\partial(\Delta u_n^z)}{\partial z} \\ \dfrac{\partial(\Delta u_n^\theta)}{r\,\partial\theta} + \dfrac{(\Delta u_n^r)}{r} \\ \dfrac{\partial(\Delta u_n^r)}{\partial z} + \dfrac{\partial(\Delta u_n^z)}{\partial r} \\ \dfrac{\partial(\Delta u_n^r)}{r\,\partial\theta} + \dfrac{\partial(\Delta u_n^\theta)}{\partial r} - \dfrac{(\Delta u_n^\theta)}{r} \\ \dfrac{\partial(\Delta u_n^\theta)}{\partial z} + \dfrac{\partial(\Delta u_n^z)}{r\,\partial\theta} \end{Bmatrix} \qquad (4\text{-}1\text{-}6)$$

and the stress-strain relationship similar to that of Eq. (2-4-8) takes the form:

$$\{\Delta\sigma\} = \begin{Bmatrix} \Delta\sigma^{rr} \\ \Delta\sigma^{zz} \\ \Delta\sigma^{\theta\theta} \\ \Delta\sigma^{rz} \\ \Delta\sigma^{r\theta} \\ \Delta\sigma^{z\theta} \end{Bmatrix} = [\,C^{ep}\,]\,\{\Delta\epsilon\}$$

$$= [C^{ep}] \sum_n \begin{Bmatrix} \Delta\varepsilon_n^{rr} \cdot \cos n\theta \\ \Delta\varepsilon_n^{zz} \cdot \cos n\theta \\ \Delta\varepsilon_n^{\theta\theta} \cdot \cos n\theta \\ \Delta\varepsilon_n^{rz} \cdot \cos n\theta \\ \Delta\varepsilon_n^{r\theta} \cdot \sin n\theta \\ \Delta\varepsilon_n^{z\theta} \cdot \sin n\theta \end{Bmatrix} = \sum_n [C^{ep}] \begin{Bmatrix} \Delta\varepsilon_n^{rr} \cdot \cos n\theta \\ \Delta\varepsilon_n^{zz} \cdot \cos n\theta \\ \Delta\varepsilon_n^{\theta\theta} \cdot \cos n\theta \\ \Delta\varepsilon_n^{rz} \cdot \cos n\theta \\ \Delta\varepsilon_n^{r\theta} \cdot \sin n\theta \\ \Delta\varepsilon_n^{z\theta} \cdot \sin n\theta \end{Bmatrix} \quad (4\text{-}1\text{-}7)$$

in which $[C^{ep}]$ is in a form with parameters of material properties $[C^e]$, H', and state of stresses $\bar{\sigma}$, $\{\sigma'\}$ as shown in Eq. (2-4-30).

4.2 Mode-mixing Characteristic

Substituting Eq. (4-1-2), (4-1-3), (4-1-4), (4-1-5), and (4-1-7) into Eq. (4-1-1), functional χ^e may be expressed as:

$$\chi^e = \int_r \int_z \int_o^{2\pi} \sum_m \sum_n \Big(\frac{1}{2} \begin{Bmatrix} \Delta\varepsilon_m^{rr} \cdot \cos m\theta \\ \Delta\varepsilon_m^{zz} \cdot \cos m\theta \\ \Delta\varepsilon_m^{\theta\theta} \cdot \cos m\theta \\ \Delta\varepsilon_m^{rz} \cdot \cos m\theta \\ \Delta\varepsilon_m^{r\theta} \cdot \sin m\theta \\ \Delta\varepsilon_m^{z\theta} \cdot \sin m\theta \end{Bmatrix}^T [C^{ep}] \begin{Bmatrix} \Delta\varepsilon_n^{rr} \cdot \cos n\theta \\ \Delta\varepsilon_n^{zz} \cdot \cos n\theta \\ \Delta\varepsilon_n^{\theta\theta} \cdot \cos n\theta \\ \Delta\varepsilon_n^{rz} \cdot \cos n\theta \\ \Delta\varepsilon_n^{r\theta} \cdot \sin n\theta \\ \Delta\varepsilon_n^{z\theta} \cdot \sin n\theta \end{Bmatrix}$$

$$- \begin{Bmatrix} \Delta u_m^r \cdot \cos m\theta \\ \Delta u_m^z \cdot \cos m\theta \\ \Delta u_m^\theta \cdot \sin m\theta \end{Bmatrix}^T \begin{Bmatrix} \Delta f_n^r \cdot \cos n\theta \\ \Delta f_n^z \cdot \cos n\theta \\ \Delta f_n^\theta \cdot \sin n\theta \end{Bmatrix} \Big) d\theta \, r\,dr\,dz - \int_\ell \int_o^{2\pi} \Big(\sum_m \sum_n \begin{Bmatrix} \Delta u_m^r \cdot \cos m\theta \\ \Delta u_m^z \cdot \cos m\theta \\ \Delta u_m^\theta \cdot \sin m\theta \end{Bmatrix}^T$$

$$\begin{Bmatrix} \Delta t_n^r \cdot \cos n\theta \\ \Delta t_n^z \cdot \cos n\theta \\ \Delta t_n^\theta \cdot \sin n\theta \end{Bmatrix} \Big) d\theta \, d\ell \quad (4\text{-}2\text{-}1)$$

It is clear that Eq. (4-2-1) is very similar to Eq. (3-2-9) except the former is in incremental form. The only difference between these two equations is that the elasto-plastic matrix $[\ C^{ep}\ ]$ is used in Eq. (4-2-1) to account for the non-linear elasto-plastic material behavior, instead of $[\ C^{e}\ ]$ in Eq. (3-2-9) for elastic analysis.

It should be noted that the elasto-plastic matrix $[\ C^{ep}\ ]$ here is actually circumferential coordinate dependent because some of its parameters, such as the deviatoric stress components $\{\sigma'\}$ and the effective stress $\bar{\sigma}$, vary along the circumferential coordinate. The orthogonality characteristics of the trigonometric functions which made it possible to simplify Eq. (3-2-9) into a sum of sub-functionals of separate modes is not applicable in this case. Separation of various modes in the formulation has thus become a problem.

4.3 Simplification of the Problem

Due to the complexity of the mode-mixing character of the problem, the analysis is now aimed at the rather simple case of structures subject only to mode 1, non-axisymmetric loads in addition to the axisymmetric loads of mode 0. Simply-supported beams of circular cross-section bent by their own weight such as CANDU reactor fuel elements, heavy pipelines, or the " Muki's problem " (canted rigid punch on a half-space) [30] are typical problems of this kind.

The incremental loading components first may be expressed as :

$$\{\Delta f\} = \{\Delta f_o\} + \begin{Bmatrix} \Delta f_1^r \cdot \cos\theta \\ \Delta f_1^z \cdot \cos\theta \\ \Delta f_1^\theta \cdot \sin\theta \end{Bmatrix} = \begin{Bmatrix} \Delta f_o^r \\ \Delta f_o^z \\ \Delta f_o^\theta \end{Bmatrix} + \begin{Bmatrix} \Delta f_1^r \cdot \cos\theta \\ \Delta f_1^z \cdot \cos\theta \\ \Delta f_1^\theta \cdot \sin\theta \end{Bmatrix} \qquad (4\text{-}3\text{-}1)$$

and

$$\{\Delta t\} = \{\Delta t_o\} + \begin{Bmatrix} \Delta t_1^r \cdot \cos\theta \\ \Delta t_1^z \cdot \cos\theta \\ \Delta t_1^\theta \cdot \sin\theta \end{Bmatrix} = \begin{Bmatrix} \Delta t_o^r \\ \Delta t_o^z \\ \Delta t_o^\theta \end{Bmatrix} + \begin{Bmatrix} \Delta t_1^r \cdot \cos\theta \\ \Delta t_1^z \cdot \cos\theta \\ \Delta t_1^\theta \cdot \sin\theta \end{Bmatrix} \qquad (4\text{-}3\text{-}2)$$

in which $\{\Delta f_o\}$, $\{\Delta t_o\}$ and $\{\Delta f_1\}$, $\{\Delta t_1\}$ are respectively the body force and surface traction of mode 0 and mode 1.

The incremental displacement components may be assumed as :

$$\{\Delta u\} = \{\Delta u_o\} + \begin{Bmatrix} \Delta u_1^r \cdot \cos\theta \\ \Delta u_1^z \cdot \cos\theta \\ \Delta u_1^\theta \cdot \sin\theta \end{Bmatrix} = \begin{Bmatrix} \Delta u_o^r \\ \Delta u_o^z \\ \Delta u_o^\theta \end{Bmatrix} + \begin{Bmatrix} \Delta u_1^r \cdot \cos\theta \\ \Delta u_1^z \cdot \cos\theta \\ \Delta u_1^\theta \cdot \sin\theta \end{Bmatrix} \qquad (4\text{-}3\text{-}3)$$

4.4 Mode-mixing Stiffness Equation

To handle the mode-mixing characteristic , $\{\Delta u\}$ is expressed in the matrix form

$$\begin{Bmatrix} \{\Delta u_0\} \\ \{\Delta u_1\} \end{Bmatrix} = \begin{bmatrix} 1 & r & z & 0 & 0 & 0 & 0 & 0 & 0 & 0 & 0 & 0 & 0 & 0 & 0 & 0 & 0 & 0 \\ 0 & 0 & 0 & 1 & r & z & 0 & 0 & 0 & 0 & 0 & 0 & 0 & 0 & 0 & 0 & 0 & 0 \\ 0 & 0 & 0 & 0 & 0 & 0 & 1 & r & z & 0 & 0 & 0 & 0 & 0 & 0 & 0 & 0 & 0 \\ 0 & 0 & 0 & 0 & 0 & 0 & 0 & 0 & 0 & 1 & r & z & 0 & 0 & 0 & 0 & 0 & 0 \\ 0 & 0 & 0 & 0 & 0 & 0 & 0 & 0 & 0 & 0 & 0 & 0 & 1 & r & z & 0 & 0 & 0 \\ 0 & 0 & 0 & 0 & 0 & 0 & 0 & 0 & 0 & 0 & 0 & 0 & 0 & 0 & 0 & 1 & r & z \end{bmatrix} \begin{Bmatrix} b_1 \\ b_2 \\ \vdots \\ b_9 \\ b_1' \\ \vdots \\ b_9' \end{Bmatrix}$$

or $$\{\Delta u\} = [\phi]_{(r,z)} \{b\} \qquad (4\text{-}4\text{-}1)$$

It should be noted that $\{b\}$ is now a 18×1 column vector instead of a 9×1 vector in Chapter III.

By a similar process given in Appendices II and III, the nodal incremental displacement components may be correlated to $\{\Delta u\}$ by :

$$\{\Delta u\}^e = [A]\{b\}$$

thus,
$$\{b\} = [A]^{-1}\{\Delta u\}^e = [h]\{\Delta u\}^e$$

and
$$\{\Delta u\} = [\phi]_{(r,z)}\{b\} = [\phi]_{(r,z)}[h]\{\Delta u\}^e$$
$$= [N]_{(r,z)}\{\Delta u\}^e \qquad (4\text{-}4\text{-}2)$$

Substituting Eq. (4-4-1) into Eq. (3-2-3), the strain-displacement relationship may be expressed as

$$\{\Delta\epsilon\} = \begin{Bmatrix} \Delta\epsilon^{rr} \\ \Delta\epsilon^{zz} \\ \Delta\epsilon^{\theta\theta} \\ \Delta\epsilon^{rz} \\ \Delta\epsilon^{r\theta} \\ \Delta\epsilon^{z\theta} \end{Bmatrix} = \begin{bmatrix} 0 & 1 & 0 & 0 & 0 & 0 & 0 & 0 & 0 & 0 & \cos\theta & 0 & 0 & 0 & 0 & 0 & 0 & 0 \\ 0 & 0 & 0 & 0 & 0 & 1 & 0 & 0 & 0 & 0 & 0 & 0 & 0 & \cos\theta & 0 & 0 & 0 & 0 \\ 1/r & 1 & z/r & 0 & 0 & 0 & 0 & 0 & 0 & \frac{\cos\theta}{r} & \cos\theta & \frac{z\cos\theta}{r} & 0 & 0 & 0 & \frac{\cos\theta}{r} & \cos\theta & \frac{z\cos\theta}{r} \\ 0 & 0 & 1/2 & 0 & 1/2 & 0 & 0 & 0 & 0 & 0 & 0 & \cos\theta/2 & 0 & \cos\theta/2 & 0 & 0 & 0 & 0 \\ 0 & 0 & 0 & 0 & 0 & 0 & 0 & 0 & 0 & \frac{-\sin\theta}{2r} & \frac{-\sin\theta}{2} & \frac{-z\sin\theta}{2r} & 0 & 0 & 0 & \frac{-\sin\theta}{2r} & 0 & \frac{-z\sin\theta}{2r} \\ 0 & 0 & 0 & 0 & 0 & 0 & 0 & 0 & 0 & 0 & 0 & 0 & \frac{-\sin\theta}{2r} & \frac{-\sin\theta}{2} & \frac{-z\sin\theta}{2r} & 0 & \sin\theta/2 & 0 \end{bmatrix} \begin{Bmatrix} b_1 \\ b_2 \\ \vdots \\ b_9 \\ b'_1 \\ \vdots \\ b'_8 \\ b'_9 \end{Bmatrix}$$

$$= [G]_{(r,z)}\{b\} \qquad (4\text{-}4\text{-}3)$$

or $$= [\,G\,]_{(r,z)}\,[\,h\,]\,\{\Delta u\}^{e}$$

$$= [\,B\,]_{(r,z)}\,\{\Delta u\}^{e} \qquad (4\text{-}4\text{-}4)$$

Substitution of Eq. (4-1-7), (4-3-1), (4-3-2), (4-4-2) and (4-4-3) into Eq. (4-1-1) and minimization of χ^{e} with respect to incremental displacement components $\{\Delta u\}^{e}$ gives a stiffness equation similar to that of Eq. (I-8) :

$$\left(\int_r\int_z\int_0^{2\pi} [B]^T[\,C^{ep}]\,[\,B\,]\,d\theta dr dz\,\right)\{\Delta u\}^{e}$$

$$= \int_r\int_z\int_0^{2\pi} [N]^T\{f\}\,r dr dz d\theta + \int_r\int_z\int_0^{2\pi}[B]^T[\,C^{e}]\{\epsilon^{o}\}(r dr dz d\theta)$$

$$+\int_{\ell'}\int_0^{2\pi}[\,N\,]^T\{\Delta t\}\;\; d\ell' d\theta \qquad (4\text{-}4\text{-}5)$$

in which $[\,C^{ep}\,]$ is given in Eq. (2-4-30).

It should be noted that the first integrands, $[B]^T[\,C^{ep}]\,[\,B\,]$ involve very complicated functions of the circumferential coordinate. Integration along the circumferential direction has to be carried out numerically. The elements of this combined matrix are given in Appendix IV.

4.5 Circumferential Integration Scheme

Integration of the stiffness matrix over the circumferential direction is carried out by the Gaussian quadrature method in this thesis. A suitable selection of the total number of Gaussian points is, of course, a compromise of accuracy and computing effort. The method itself states that :

$$\int_0^{2\pi} \left(\int_r \int_z [\,B\,]^T [\,C^{ep}\,][\,B\,]\, r\,dr\,dz \right) d\theta$$

$$= \sum_{k=1}^{N} \left[A_k \int_r \int_z \left([\,B\,]^T [\,C^{ep}\,][\,B\,] \right)_{(\theta_k)} r\,dr\,dz \right] \qquad (4\text{-}5\text{-}1)$$

in which A_k are the weighting factors of Gaussian quadrature, N is the total number of Gaussian points evaluated, θ_k are the individual Gaussian points along the circumferential direction and the integrand $[\,B\,]^T[\,C^{ep}\,][\,B\,]$ is a 18 x 18 matrix, which has to be formulated term-by-term before the integration. The detailed formulation of $[\,B\,]^T[\,C^{ep}\,][\,B\,]$ may be found in Appendix IV.

4.6 Special Discussion on the Circumferential Integration Scheme for the Stiffness Matrix

The integration of the stiffness matrix of Eq. (4-5-1) along the circumferential direction is carried out by the Gaussian quadrature method as described above. The method evaluates values of the integrand $[B]^T[C^{ep}][B]$ only at those selected Gaussian points θ_k. It is quite clear that the integration scheme is actually an approximating process,not only from the mathematical point of view (i.e. evaluate integration by summation), but also from the material behavior point of view. The parameters of the non-linear elasto-plastic material behavior such as H', $\bar{\sigma}$, $\{\sigma'\}$, etc., are evaluated only at those selected N Gaussian points θ_k. As a matter of fact, the decision in selecting the total number of Gaussian

points determines the integration accuracy from both the mathematical and material behaviour points of view.

CHAPTER V

COMPUTER CODE AND CASE STUDIES

5.1 Computer Code " NTEPSA "

A computer code by the name of " NTEPSA " was developed to incorporate the theory described in Chapter IV. Another code " NLSTRS " described earlier in Chapter III for the elastic analysis was used as the basis for this development . Simulation of the non-linear elasto-plastic material behavior was added to this new code using the stepwise linear incremental method as described in Chapter II (for which another code " TEPSA " is available for the elasto-plastic analysis of axisymmetric structures under axisymmetric loads [3]). As described in Chapter IV, the present analysis is aimed at problems of axisymmetric structures subject to mode 1 non-axisymmetric loads only, in addition to the axisymmetric loads of mode 0.

It should also be noted that a total number of nine Gaussian points were used in this code for the integration procedure along the circumferential direction. It was, of course, a compromise between the integration accuracy and computing effort.

5.2 Sample Problem

The problem of a simply supported heavy tube(4" O.D.,3" I.D., 16" long) bent by its own weight is chosen as a sample problem.

This problem is almost the same as the sample problem of a heavy beam described in Appendix III for the elastic analysis. The reason for choosing a tube instead of a beam in this elasto-plastic analysis was that a tube needs fewer nodes and elements in the finite element discretization, and thus reduces the computing effort. In the present analysis, a finite element discretization consisting 18 nodes and 8 elements was used. The detailed configuration of the tube and its discretization are shown in Figure 11.

The loading condition of the sample problem consists of only mode 1, non-axisymmetric load as described in Appendix III. However, in order to demonstrate the mode-mixing characteristic , an incremental longitudinal tensile force was imposed at both ends of the tube to account for the axisymmetric load (mode 0). Thus, the sample problem is essentially just like a heavy tube undergoing a tensile test horizontally. The solutions of the sagging and bending stress of the tube due to its own weight at various stress states during the tensile test are the main interest, besides the axisymmetric solutions of longitudinal elongation, tensile stress and strain. It should also be noted that other problems such as a heavy tube horizontally mounted under internal or external pressure (e.g. large gas pipelines or CANDU fuel elements, for example) are relevent sample problems as well.

5.3 Verification of Computer Code " NTEPSA "

Generally, verification of a new computer code is done by comparing the output obtained from the code with experimental data, analytical solutions, or solutions obtained from an established computer code, for various sample problems. However, in the present analysis, only a specified category of problems (axisymmetric solids subject to mode zero and mode one loads) is intended and no experimental data, analytical solutions, or solutions obtained from an established computer code for this kind of problems are available to the author. Verification of " NTEPSA " can only be done, for the time being, by comparing the outputs from the code for the above sample problem with outputs from two of its base codes " NLSTRS " and " TEPSA ". As described before, " NLSTRS " is a code for the elastic analysis of axisymmetric structures subject to non-axisymmetric loading by the combined finite element and Fourier expansion method. Verification of the " NLSTRS " code may be found in Appendix III (or Table 1 for easy reference). The other base code " TEPSA " is a code for the elasto-plastic analysis of axisymmetric structures subject to axisymmetric loading by the linear incremental method, which has been verified in many publications, such as Ref.[3]. The results of the verification are described as follow :

(i) Verification of " NTEPSA " with " NLSTRS "

Within the elastic range of material behavior, solutions of suitable sample problems obtained from both codes should be identical. The sample problem of a heavy tube described in this chapter was calculated by both codes. The material properties of the tube were assigned to be :

$E = 0.28 \times 10^8$ -----Young's Modulus

$\rho = 0.33$ -----Poisson's ratio

The density of the tube, ρ, was assigned to be 22.5, 50, and 100 $lbf/in.^3$ respectively at three runs. Computer outputs of saggings and bending stresses from both codes have been tabulated in Table 2. It shows excellent agreement between the solutions obtained from both codes. Solutions obtained by simple beam theory are also indicated in this Table for reference.

(ii) Verification of " NTEPSA " with " TEPSA "

It is quite clear that code " NTEPSA " should yield the same results on the elasto-plastic analysis as code " TEPSA " for problems which involve only axisymmetric loads. The sample problem described in this chapter is a suitable one if the density of the tube material becomes negligible (e.g. 0.0001 $lbf/in.^3$). Solutions of axial strain, axial stress and radial deformation from both codes have been tabulated in Table 3. Good agreement of solutions from both codes is also attained. Material properties used for input to the computations

were :

$E = 0.28 \times 10^8$ psi ------- Young's modulus

$\nu = 0.33$ ------- Poisson's ratio

$\sigma_y = 40{,}000.$ psi ------- yield stress

$E' = 40{,}000.$ psi ------- asymptot. modulu

$\sigma_k = 41{,}000.$ psi ------- sigma bi-linear kink

$n = 5.$ ------- stress power

for both codes.

5.4 Case Study - An Elasto-plastic Analysis of the Sample Problem by " NTEPSA " Code

The behavior of a simply supported tube subject to longitudinal tensile force which sags due to its own weight was assessed by the " NTEPSA " code. The discretization of the finite element model remained the same as shown in Figure 11. The elasto-plastic material behavior was illustrated in Figure 12, or by the following parameters:

$E = 0.28 \times 10^8$ psi -------Young's modulus

$\nu = 0.33$ -------Poisson's ratio

$\sigma_y = 40{,}000.$ psi -------yield stress

$E' = 40{,}000.$ psi -------asymptot modulus

$\sigma_k = 40{,}000.$ psi -------sigma bi-linear kink

$n = 5.$ -------stress power

according to Eq. (2-4-31).

As described before, the main purpose of this case study is to assess the validity of the combined finite element and Fourier expansion method for the elasto-plastic analysis of axisymmetric structures subject to non-axisymmetric loadings. The following information on the deformation of the tube due to the non-axisymmetric loads are of main interest.

(i) The radial and tangential deformations of the tube due to the non-axisymmetric load at 3.94% effective strain as shown in Figure 13.

(ii) The sagging of the tube along longitudinal direction at various angular positions at 3.94% effective strain as shown in Figure 14.

(iii) The deformed shape of the mid-span cross-section of the tube at 3.94% effective strain as shown in Figure 15. It should be noticed that the deformations have been exaggerated in the figure.

(iv) The sagging of the tube at various states of stress (or strain) is shown in Figure 16. The figure indicates that the sagging of the tube accelerates when the elastic limit of the material is exceeded.

CHAPTER VI

DISCUSSION AND CONCLUSIONS

6.1 Discussion

Although the present "NTEPSA" code has been indirectly verified by two special loading situations from two of its base codes "NLSTRS" and "TEPSA" as described in Chapter V, the validity of the elasto-plastic version of the code for the general loading situation has not yet been verified directly. Direct verification of the code for general application can be achieved if experimental data or solutions obtained from an established three-dimensional elasto-plastic finite element program are available. Unfortunately, these data are not accessible to the author for the time being. Hence a full verification of this code was not possible at this time.

The analysis and the "NTEPSA" code described in this thesis are intended to be a preliminary study of the combined finite element and Fourier expansion method for the elasto-plastic analysis of axi-symmetric structures subject to general non-axisymmetric loadings. It is important at this stage to assess whether further research activity in this area should be recommended.

As mentioned earlier, the main advantage of the application of this combined finite element and Fourier expansion method over the general three-dimensional finite element method is in the potential savings in computer input data, computing effort and storage. Comparison between these two approaches can be demonstrated by the sample problem illustrated in Fig.11. Information, including the

total number of nodes and elements required, in the size of the overall stiffness matrix and the total number of integrations by using the Gaussian quadrature scheme for both methods, is tabulated in Tables 3 and 4 for direct comparison. It should be noted that, for a three-dimensional finite element program, every toroidal element used in the present analysis has to be divided into a number of hexahedral elements. In Table 4 and Table 5, a total of nine such elements would be needed for a three-dimensional finite element analysis.

In Table 4, it can be seen that the " NLSTRS " code (i.e., the combined finite element and Fourier expansion method for elastic analysis) can achieve a five times saving in the amount of required input data, an eighty-one times saving in the amount of required storage and a ninety-six times saving in the amount of required computing effort.

In Table 5, it also can be seen that the " NTEPSA " code (i.e., the combined finite element and Fourier expansion method for elasto-plastic analysis) can achieve a five times saving in the amount of required input data, a twenty times saving in the amount of required storage and a three times saving in the amount of required computing effort.

Referring to Tables 4 and 5, a considerable saving is achieved by both " NLSTRS " and " NTEPSA " codes. However, it also reveals a drastic decrease in the savings of storage and computing effort required for the elasto-plastic analysis. The savings may become less if more modes are included in the analysis. Table 6

reveals that the amount of required computing effort is even more for the combind finite element and Fourier expansion method if four modes are included. Nevertheless, the saving in the amount of input data and the computing effort required to solve the stiffness equation (because of the smaller size of stiffness matrix) still make the method more competitive over the general three-dimensional finite element method, provided that four or five loading modes can satisfactorily represent the loading situation of the problem.

The above comparison didnot include the effort required for the thermal analysis. While almost all three-dimentional thermal analysis codes have been based on the finite difference method because of its effectiveness, the combined finite element and Fourier expansion approach has already been established [12]. It is believed that the gain in using the present method for coupled thermoelasto-plastic analysis over an equivalent three-dimensional finite element analysis would be even more phenomenal.

Besides the above mode-mixing limitation, there are two other main factors which may also affect the feasibility of the application of the combined finite element anf Fourier expansion method. One of the factors is the convergence of solutions with the mesh size of the finite element discretization. The other is the integration accuracy of the Gaussian quadrature scheme used in the " NTEPSA " code.

In Table 7, solutions of the sagging for the sample problem illustrated in Fig.11-a by " NTEPSA " code, using three finite element discretizations of different mesh sizes, have been tabulated for comparison. These three finite element discretizations are illustrated in Fig.11-b,

Fig. 17-a and 17-b. It can be seen that the solution for the eight-element discretization (shown in Fig. 11-b) and that for the sixteen-element discretization (shown in Fig. 17-b) are very close. It appears that the solution does converge with the mesh size of the discretization and the rather simple finite element discretization as shown in Fig. 11-b is able to represent the structural behavior of the sample problem satisfactorily.

As for the integration accuracy of the Gaussian quadrature scheme, many references such as Ref. [14] are available for assessing the required Gaussian integration points to obtain satisfactory accuracy of integration over a plane triangular element. However, in the "NTEPSA" code, integrands of elements of the stiffness matrix (as shown in Appendix IV) are circumferential coordinate dependent. Integration of these elements over the circumferential coordinate has to be specially discussed. Referring to Appendix IV, it can be seen that these integrands can be classified into three categories, namely,

$$I_1 = a_1/(b_1\cos^2\theta + b_2\cos\theta\sin\theta + b_3\sin^2\theta)$$

$$I_2 = (a_1\cos\theta + a_2\sin\theta)/(b_1\cos^2\theta + b_2\cos\theta\sin\theta + b_3\sin^2\theta)$$

$$I_3 = (a_1\cos^2\theta + a_2\sin^2\theta + a_3\sin\theta\cos\theta)/(b_1\cos^2\theta + b_2\cos\theta\sin\theta + b_3\sin^2\theta)$$

where a_1, a_2, a_3, b_1, b_2, b_3 are various constants for various integrands. In Table 8, it can be seen that the Gaussian quadrature scheme with nine integration points appeared to give reasonably accurate results, e.g. to the order of 10^{-3} for the integrand I_2 .

6.2 Conclusions

From the analysis and case studies described in this thesis, it may be concluded that:

(1) Within the elastic limit, the combined finite element and Fourier expansion method has proved to be capable of solving problems of axisymmetric structures subject to non-axisymmetric loadings. Compared to the simple beam theory, the method affords a complete and accurate set of three-dimensional displacement,strain and stress solutions. This method achieves a five times saving in the amount of required input data when it is compared with a general three-dimensional finite element program, an eighty-one times saving in the amount of required storage and a ninety-six times saving in the amount of required computing effort.

(2) For the elasto-plastic analysis, the mode-mixing characteristic of the method somewhat restricts practical application of the method for general loading conditions. Four or five loading modes appears to be the limiting factor of this method when competing with a general three-dimensional F.E. elasto-plastic finite element program.

(3) The case study of a simply supported tube subject to longitudinal tensile loads sagging under its own weight with the " NTEPSA " code reveals an increasing sagging of the tube as the material behavior of the tube goes through the elasto-plastic region (as shown in Figure 16). As expected, the tube cross-section no longer was round (as shown in Figure 14 and 15) after deformation.

The "induced sagging" of the tube by the effect of material plasticity may be predicted by idealized plastic simple beam theory, but solutions of the deformed cross-sections of the tube can only be obtained by this combined finite element and Fourier expansion method or a three-dimensional elasto-plastic finite element method.

(4) It should be noted that,in both "NLSTRS" and "NTEPSA" codes, rotations are not considered to be degrees of freedom in the analysis. Both codes are thus valid only for small strain problems. It should also be noted that,although "NTEPSA" code has been indirectly verified by two of its base codes,"NLSTRS" and "TEPSA",direct verification of the code with experimental data or solutions obtained from a verified three-dimensional elasto-plastic finite element program is recommended.

leaf blank to correct numbering

REFERENCES

[1] Turner, M. J., Clough, R. W., Martin, H. C., and Topp, L. J., " Stiffness and Deflection Analysis of Complex Structures", Journal of Aeronautical Science 23, pp. 805-823,(1956).

[2] Proceedings of the Wright-Patterson Conferences on Matrix Methods in Structural Analysis, First Conference (1951) and Second Conference (1968), Dayton, Ohio.

[3] Hsu, T. R., Bertels,A. W. M., Arya, B., and Banerjee, S., "Application of the Finite Element Method to the Non-linear Analysis of Nuclear Reactor Fuel Behavior" in Computational Methods in Nonlinear Mechanics ed. by J. T. Oden et al, TICOM Press (1974), pp. 531-540.

[4] Nayak, G. C. and Zienkiewicz, O. C., "Elsato-plastic Stress Analysis, A Generalization for Various Contitutive Relations Including Strain Softing", Int. J. Num. Meth. Engng 5, pp. 113-115(1972).

[5] "Thermal Structural Analysis Program - A Survey & Evaluation", Hold as part of the Third Annual Pressure Vessels and Piping Conference, and 27th Annual Petroleum-Mechanical Eng. Conference, Sep. (1972), New Oreans, La.

[6] Fenves, Perrone, Robinson and Schnobrich, " Numerical and Computer Methods in Structural Mechanics ", Academic Press, N. Y. and London, (1973).

[7] Gallagher, R. H., Yamada Y., and Oden, J. T. (eds.) " Recent Advances in Matrix Methods in Structural Analysis & Design ", First Japan-United States Seminar on Matrix Methods of Structural Analysis and Design, Tokyo, 1969.

[8] Gupta, A. K. , Mohraz, B. and Schnobrich, W. C., "Elasto-plastic Analysis of Three-dimensional Structures Using the Isoparametric Element ", Report No. UILU-ENG-71-2020, Univ. of Ill., Urbana, Ill.,(1971).

[9] Levy, N., Marcal, P. V., and Rice, J. R., " Progress in Three-dimensional Elastic-plastic Stress Analysis for Fracture Mechanics ",J.Nucl. Eng. Design, 17, pp. 64-75 (1971).

[10] Owen D. R. J., and Salonen, E. M. ," Three-dimensional Elasto-plastic Finite Element Analysis ", International Journal for Num. Methods in Eng. Vol. 9, pp. 209-218 (1975).

[11] Desai, C. S., and Abel, J. F., " Introduction to the Finite Element Method - A Numerical Method dor Engineering Analysis ", Van Nostrand Reinhold Company, N. Y. (1972), pp. 285-302.

[12] Wilson, E. L., " Structural Analysis of Axisymmetric Solids ",AIAA J. Vol. 3, No. 12 (Dec. 1965).

[13] Percy, J. H., Piam, T. H. H., Klein, S., and Navaratna, D. R., " Application of the Matrix Displacement Method to Linear Elastic Analysis of Shells of Revolution ", AIAA J. Vol. 3, No. 11 (Nov. 1965).

[14] Zienkiewicz, O. C., "The Finite Element Method in Engineering Science", McGraw-Hill, London, England.

[15] Martin, H. C., and Carey, G. F., " Introduction to Finite Element Analysis - Theory and Application ", McGraw-Hill press, N. Y., (1973).

[16] Padlog, J., Huff, R. D., and Holloway, G. F., " The Inelastic Behaviour of Structures Subjected to Cyclic, Thermal and Mechanical Stressing Conditions", Bell Aerosystems Co. Rept. WPADD TR60-271,(1960).

[17] Swedlow, J. L., and Yang, W. H.: Stiffness Analysis of Elastic-plastic Plates, Grad. Aeron. Lab., Calif. Inst. Technol.SM65-10, (1965).

Pope, G., " A Discrete Element Method for Analysis of Plane Elastic -plastic Stress Problems", Roy. Aeron. Estab. TR65028, (1965).

[18] Proc. 3rd Conf. Matrix Methods Struct. Mech., Wright-Patterson AFB, Ohio, (Oct. 1971).

[19] Oden, J. T., Clough, R. W., and Yamamoto, Y. (eds.), " Advances in Computational Methods in Structural Mechanics and Design " Proc. 2nd United States-Japan Seminar Matrix Methods of Struct. Analysis and Design, Calif., (Aug. 1972), Univ. of Alabam press, (1972).

[20] Yamada, Y., " Recent Advances in Matrix Methods of Structural Analysis and Design ", pp. 283-316, Reference [7].

[21] Zienkiewicz, O. C., Valliappan, S. and King, I. P., "Elasto-plastic Solutions of Engineering Problems 'Initial Stress', Finite Element Approach ", Int. J. num. Meth. Engng Vol. 1, pp. 75-100, (1969).

[22] Marcal, P. V. and King, I. P., " Elastic-plastic Analysis of Two-dimensional Stress Systems by the Finite Element Method ", Int. J. Meth. Sci., Pergamon press Ltd., (1967), Vol. 9, pp. 143-155.

[23] Boyle, E. F. and Jennings, A., " Accelerating the Convergence of Elasto-plastic Stress Analysis ", Int. J. num. Meth. Engng, pp. 232-235, Vol. 6, (1972).

[24] Clough, R. W. and Rashid, Y., " Finite Element Analysis of Axisymmetric Solids ", Journal of ASCE, Engineering Mechanical Division, Vol. 91, No. EM-1 (1965).

[25] Dunham, R. S. and Nickell, R. E., " Finite Element Analysis of Axisymmetric Solids with Arbitrary Loadings ", Structural Engineering Lab. Report 67-6, University of Calif., Berkeley (1967).

[26] as Reference [1], pp. 263.

[27] Zienkiewicz, O. C. and Too, J. J. M., " The Finite Prism in Analysis of Thick Simply Supported Bridge Boxes ", Proc. Instn. Civ. Engrs, 1972, 53 (Sep.), pp. 147-172 (1972).

[28] Doherty, W. P. and Wilson, E. L., and Taylor, R. L., " Stress Analysis of Axisymmetric Solids Utilizing Higher Order Quadrilateral Finite Elements ", Structural Engineering Lab. Report 69-3, Universtiy of Calif., Berkely (1969)

[29] Zienkiewicz, O. C., " Isoparametric and Allied Numerically Integrated Elements ", Int. Symp. on Num. and Computer Methods in Struct. Mech., University of Illinois, Urbana, 1971.

[30] Ricardo Nicolau del Roure, " Evalution of Low Order Axisymmetric Finite Elements with Fourier Loadings ", Master Thesis, Dept. of Civil Eng., the Univ. of Texas, at Austin.

[31] Ueda, Y. and Yamakama, T., " Thermal Nonlinear Behaviour of Structures ", appeared in the Symposium Volume of Ref. 19 , pp. 375-392.

[32] Yamada, Y. and Yoshimura N. and Sakurai, T., " Plastic Stress-strain Matrix and Its Application for the Solution of Elastic-Plastic Problems by the Finite Element Method " Int. J. of Mech. Sci., Pergamon Press, Vol. 10, 1968, pp. 343-354.

[33] Gallagher, R. H., " Computational Methods in Nuclear Reactor Structural Design for High Temperature Application : An Interpretive Report ", Oak Ridge National Lab., Report ORNL 4756, (Feb. 1973).

[34] Hsu, T. R., Bertels, A. W. M., Banerjee, S., and Harrison, W. C. " Theoretical Basis for a Transient Thermal Elasto-plastic Stress Analysis of Nuclear Reactor Fuel Elements" Whiteshell Nuclear Research Establishment, Report AECL-5233, Atomic Energy of Canada, (July, 1976).

[35] Popov, E. P., " Introduction to Mechanics of Solids ", Englewood Cliffs, Prentice-Hall (1968).

[36] as Ref. [34] , pp. 29-30.

[37] Pearson, karl, " On The Flexure of Heavy Beams Subjected to Continuous Systems of Load", Quarterly Journal of Pure and Applied Mathematics, Vol. 24 & 31, 1889, pp.63.

[38] Roark, Raymond J., " Formulas for Stress and Strain ", McGraw-Hill Book Company, 1965, pp106.

APPENDIX I

Stiffness of Torus Elements

(i) Detailed Formulation of The Stiffness Equation of a Constant Strain Triangular Torus Element under Axisymmetric Loading :

Because of the characteristics of axisymmetry of the element geometry and loadings, the displacement components for the element may be assumed to be independent of the circumferential coordinate, i.e.

$$\{u\} = \begin{Bmatrix} u_{r(r,z)} \\ u_{z(r,z)} \end{Bmatrix} = \begin{Bmatrix} b_1 + b_2 r + b_3 z \\ b_4 + b_5 r + b_6 z \end{Bmatrix}$$

or

$$\{u\} = \begin{bmatrix} 1 & r & z & 0 & 0 & 0 \\ 0 & 0 & 0 & 1 & r & z \end{bmatrix} \begin{Bmatrix} b_1 \\ b_2 \\ b_3 \\ b_4 \\ b_5 \\ b_6 \end{Bmatrix} = \left[\phi_{(r,z)}\right] \{b\} \qquad \text{(I-1)}$$

in the matrix and vector forms, in which $[\ ]$, $\{\ \}$ represent matrix and vector respectively and $b_1, b_2, \ldots\ldots, b_6$ are arbitary constants.

The nodal values of this assumed displacement pattern at nodes I, J, K as shown in Figure 2, may be expressed as :

$$\begin{Bmatrix} u^e_{r,I} , u^e_{z,I} \\ u^e_{r,J} , u^e_{z,J} \\ u^e_{r,K} , u^e_{z,K} \end{Bmatrix} = \begin{bmatrix} 1 & r_i & z_i \\ 1 & r_j & z_j \\ 1 & r_k & z_k \end{bmatrix} \begin{Bmatrix} b_1 & b_4 \\ b_2 & b_5 \\ b_3 & b_6 \end{Bmatrix}$$

or

$$\{u\}^e = [A]\{b\} \qquad \text{(I-2)}$$

Inversion of Eq. (I-2) yields :

$$\{b\} = [A]^{-1}\{u^e\} = [h]\{u^e\} \qquad \text{(I-3)}$$

in which

$$[h] = [A]^{-1} = \frac{1}{\beta}\begin{bmatrix} r_j z_k - r_k z_j & r_k z_i - r_i z_k & r_i z_j - r_j z_i \\ z_j - z_k & z_k - z_i & z_i - z_j \\ r_k - r_j & r_i - r_k & r_j - r_i \end{bmatrix} \qquad \text{(I-4)}$$

and $\beta = r_j(z_k - z_i) + r_i(z_j - z_k) + r_k(z_i - z_j)$

The pattern (or usually refered as " interpolation function ") which was assumed in Eq. (2-3-3) to correlate the displacement vector $\{u\}$ with its nodal values $\{u\}^e$ is obtained by

$$\{u\} = [\phi_{(r,z)}]\{b\}$$
$$= [\phi_{(r,z)}] \cdot [h]\{u\}^e \qquad \text{(I-5)}$$

or simply

$$\{u\} = \left[N_{(r,z)}\right] \{u\}^e \qquad \text{(I-6)}$$

with $\left[N_{(r,z)}\right] = \left[\phi_{(r,z)}\right]\left[h\right]$

Substitute Eq. (I-1) into Eq. (2-3-5) of the strain-displacement relation, one obtains :

$$\{\epsilon\} = \begin{Bmatrix} \epsilon_{rr} \\ \epsilon_{zz} \\ \epsilon_{\theta\theta} \\ \epsilon_{rz} \end{Bmatrix} = \begin{Bmatrix} \frac{\partial u_r}{\partial r} \\ \frac{\partial u_z}{\partial z} \\ \frac{u_r}{r} \\ \frac{\partial u_r}{\partial z} + \frac{\partial u_z}{\partial r} \end{Bmatrix} = \begin{Bmatrix} b_2 \\ b_6 \\ \frac{b_1 + b_2 r + b_3 z}{r} \\ b_3 + b_5 \end{Bmatrix}$$

or in matrix form as :

$$\{\epsilon\} = \begin{bmatrix} 0 & 1 & 0 & 0 & 0 & 0 \\ 0 & 0 & 0 & 0 & 0 & 1 \\ \frac{1}{r} & 1 & \frac{z}{r} & 0 & 0 & 0 \\ 0 & 0 & 1 & 0 & 1 & 0 \end{bmatrix} \begin{Bmatrix} b_1 \\ b_2 \\ b_3 \\ b_4 \\ b_5 \\ b_6 \end{Bmatrix}$$

$$= \left[G_{(r,z)}\right] \{b\}$$
$$= \left[G_{(r,z)}\right] \left[h\right] \{u\}^e$$
$$= \left[B\right] \{u\}^e \qquad \text{(I-7)}$$

with $\left[B_{(r,z)}\right] = \left[G_{(r,z)}\right] \left[h\right]$

The stiffness equation of a typical element as shown in Eq. (2-3-8), (2-3-9), and (2-3-10), or :

$$\left(\int_{V'} [B]^T [C^e][B]\, dV'\right)\{u\}^e = \int_{V'} [N]^T \{f\}\, dV' + \int_{V'} [B]^T [C^e]\{\epsilon_o\}\, dV' + \int_{S'} [N]^T \{t\}\, dS' \quad \text{(I-8)}$$

may now be established as :

$$\left([h]^T \int_{V'} [G_{(r,z)}]^T [C^e][G_{(r,z)}]\, dV' [h]\right).\{u\}^e = [h]^T \int_{V'} [\phi_{(r,z)}]\{f\}\, dV' + [h]^T \int_{V'} [G_{(r,z)}][C^e]\{\epsilon_o\} dV' + [h]^T \int_{S'} [\phi_{(r,z)}]\{t\}\, dS' \quad \text{(I-9)}$$

The integrands in the first integral of Eq. (I-9), after expansions, take the form :

$$[G]^T[C^e][G] = \begin{bmatrix} \frac{1}{r^2}C_{33} & \frac{1}{r}(C_{31}+C_{33}) & \frac{z}{r^2}C_{33}+\frac{1}{r}C_{34} & 0 & \frac{1}{r}C_{34} & \frac{1}{r}C_{32} \\ & C_{11}+C_{13}+C_{33}+C_{31} & \frac{z}{r}(C_{13}+C_{33})+C_{14}+C_{34} & 0 & C_{14}+C_{34} & C_{12}+C_{32} \\ & & \frac{z^2}{r^2}C_{33}+\frac{z}{r}(C_{34}+C_{43})+C_{44} & 0 & \frac{z}{r}C_{34}+C_{44} & \frac{z}{r}C_{32}+C_{42} \\ & \text{(Symmetrical)} & & 0 & 0 & 0 \\ & & & & C_{44} & C_{42} \\ & & & & & C_{22} \end{bmatrix}$$

(ii) Numerical Integration of Integrands over the Volume V' and Boundary Surface S' of a Triangular Torus Element :

The stiffness equation (I-9) involves integration of certain integrands over the volume V' and boundary surface S' of a typical triangular torus element as shown in Fig. 2. The following types of integrations have to be calculated in the finite element analysis :

$$I_1 = \int_{V'} f(r,z) \; dV' \qquad \text{(I-10a)}$$

$$I_2 = \int_{S'} g(r,z) \; dS' \qquad \text{(I-10b)}$$

These integrals may be expressed in the cylindrical coordinate system as :

$$I_1 = \int_r \int_z \int_\theta f(r,z) \; (r \; dr \; dz \; d\theta \;) = 2\pi \int_r \int_z f(r,z) (r dr dz) \qquad \text{(I-11a)}$$

$$I_2 = \int_{\ell'} \int_\theta g(r,z) \; d\ell' \; d\theta = 2\pi \int_{\ell'} g(r,z) \; d\ell' \qquad \text{(I-11b)}$$

in which $d\ell'$ represents increment of path length along the element boundary of the finite element grid on the r - z plane.

Equation (I-11b) may be simply approximated as

$$I_2 = \bar{g} \; (r,z) \; \ell'$$

in which $\bar{g}\,(r,z)$ is the algebraic average of $g(r,z)$ along boundary ℓ' .

Exact integration of Eq. (I-11a) is possible but is both tedious and time consumming. In this thesis, the Gaussian quadrature numerical integration scheme is used. The scheme uses n "Gaussian points " and arrives at a summation expression with appropriate weighting coefficients at each Gaussian point, or :

$$I_2 = \sum_{i=1}^{n} \sum_{j=1}^{n} W_{ij} \; f(r_i, z_j)$$

Details of the scheme may be found in many references such as Ref. [14].

APPENDIX II

Stiffness of a Torus Element Subject to Non-axisymmetric Load

Detailed Formulation of the Stiffness Equation of a Constant Strain Triangular Torus Element under Non-axisymmetric Loadings :

Similar to Eqs.(2-3-8), (2-3-9), and (2-3-10), the stiffness equation for the problem is

$$\left(\int_r\int_z \left(\left[B_n\right]^T\left[C^e\right]\left[B_n\right]\ (\ r\ dr\ dz\ )\right)\left\{u_n\right\}^e = \int_r\int_z \left[N\right]\left\{f_n\right\}\ (rdrdz) + \int_r\int_z \left[B_n\right]^T\left[C^e\right]\left\{\epsilon_n^0\right\}\ (\ rdrdz\ ) + \int_{\ell'}\left[N\right]\left\{t_n\right\}\ d\ell\ ' \qquad \text{(II-1)}$$

for each mode n .

Assuming that the displacement components $\{u_n\}$ for mode n are given by :

$$\left\{u_n\right\}(r,z) = \begin{Bmatrix} u_n^r \\ u_n^z \\ u_n^\theta \end{Bmatrix} = \begin{bmatrix} 1 & r & z & 0 & 0 & 0 & 0 & 0 & 0 \\ 0 & 0 & 0 & 1 & r & z & 0 & 0 & 0 \\ 0 & 0 & 0 & 0 & 0 & 0 & 1 & r & z \end{bmatrix} \begin{Bmatrix} b_{1n} \\ b_{2n} \\ b_{3n} \\ b_{4n} \\ b_{5n} \\ b_{6n} \\ b_{7n} \\ b_{8n} \\ b_{9n} \end{Bmatrix} \qquad \text{(II-2)}$$

or $\left\{u_n\right\}(r,z) = \left[\phi_{(r,z)}\right]\left\{b_n\right\}$

Similar to Eq. (I-2), the nodal values of the displacement components $\{u_n\}^e$ may be related to b_n as :

$$\begin{Bmatrix} u^r_{nI} & u^z_{nI} & u_{nI} \\ u^r_{nJ} & u^z_{nJ} & u_{nJ} \\ u^r_{nK} & u^z_{nK} & u_{nK} \end{Bmatrix} = \begin{bmatrix} 1 & r_i & z_i \\ 1 & r_j & z_j \\ 1 & r_k & z_k \end{bmatrix} \begin{Bmatrix} b_{1n} & b_{4n} & b_{7n} \\ b_{2n} & b_{5n} & b_{8n} \\ b_{3n} & b_{6n} & b_{9n} \end{Bmatrix}$$

or $$\{u_n\}^e = [A]\{b_n\} \qquad \text{(II-3)}$$

Inverse (II-3), one obtains :

$$\{b_n\} = [h]\{u_n\}^e$$

with $$[h] = [A]^{-1}$$

$$= \frac{1}{\Delta} \begin{bmatrix} r_j z_k - r_k z_j & 0 & 0 & r_k z_i - r_i z_k & 0 & 0 & r_i z_j - r_j z_i & 0 & 0 \\ z_j - z_k & 0 & 0 & z_k - z_i & 0 & 0 & z_i - z_j & 0 & 0 \\ r_k - r_j & 0 & 0 & r_i - r_k & 0 & 0 & r_j - r_i & 0 & 0 \\ 0 & r_j z_k - r_k z_j & 0 & 0 & r_k z_i - r_i z_k & 0 & 0 & r_i z_j - r_j z_i & 0 \\ 0 & z_j - z_k & 0 & 0 & z_k - z_i & 0 & 0 & z_i - z_j & 0 \\ 0 & r_k - r_j & 0 & 0 & r_i - r_k & 0 & 0 & r_j - r_i & 0 \\ 0 & 0 & r_j z_k - r_k z_j & 0 & 0 & r_k z_i - r_i z_k & 0 & 0 & r_i z_j - r_j z_i \\ 0 & 0 & z_j - z_k & 0 & 0 & z_k - z_i & 0 & 0 & z_i - z_j \\ 0 & 0 & r_k - r_j & 0 & 0 & r_i - r_k & 0 & 0 & r_j - r_i \end{bmatrix}$$

and $\lambda = r_i(z_j - z_k) + r_j(z_k - z_i) + r_k(z_i - z_j)$ (II-4)

Matrix $[N]$ may be now formulated by

$$[N] = [\phi_{(r,z)}][h] \qquad \text{(II-5)}$$

Substitute Eq. (II-2) into Eq. (3-2-3) of the strain-displacement relation, one obtains :

$$\{\epsilon_n\} = \begin{Bmatrix} \epsilon_n^{rr} \\ \epsilon_n^{zz} \\ \epsilon_n^{\theta\theta} \\ \epsilon_n^{rz} \\ \epsilon_n^{r\theta} \\ \epsilon_n^{z\theta} \end{Bmatrix} = \begin{bmatrix} 0 & 1 & 0 & 0 & 0 & 0 & 0 & 0 & 0 \\ 0 & 0 & 0 & 0 & 0 & 1 & 0 & 0 & 0 \\ 1/r & 1 & 1/z & 0 & 0 & 0 & n/r & n & nr/r \\ 0 & 0 & 1 & 0 & 0 & 0 & 0 & 0 & 0 \\ -n/r & -n & -nz/r & 0 & 0 & 0 & -1/r & 0 & -z/r \\ 0 & 0 & 0 & -n/r & -n & -nr/z & 0 & 0 & 1 \end{bmatrix} \begin{Bmatrix} b_{1n} \\ b_{2n} \\ b_{3n} \\ b_{4n} \\ b_{5n} \\ b_{6n} \\ b_{7n} \\ b_{8n} \\ b_{9n} \end{Bmatrix}$$

or $\{\epsilon_n\} = [G_n]_{(r,z)}\{b_n\}$

Matrix $[B_n]$ may now be formulated by

$$[B_n] = [G_n]_{(r,z)}[h] \qquad \text{(II-6)}$$

Finally, integrands $[G_n]^T_{(r,z)}[C^e][G_n]_{(r,z)}$ in the stiffness equation, after expansion, takes the form :

$$[G_n]_{(r,z)}[C^e][G_n]_{(r,z)} =$$

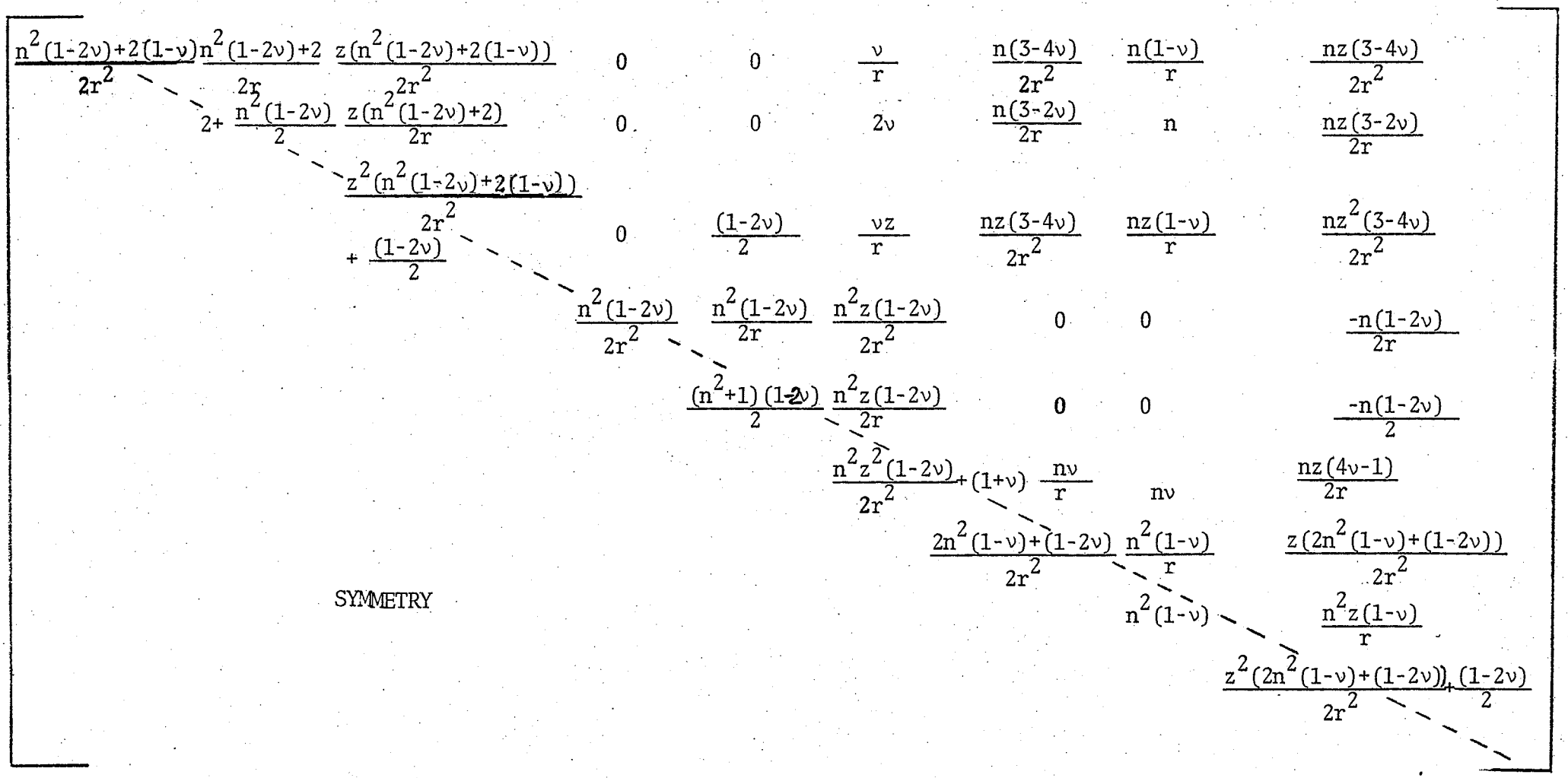
$\frac{n^2(1-2\nu)+2(1-\nu)}{2r^2}$
$\frac{n^2(1-2\nu)+2}{2r}$
$\frac{z(n^2(1-2\nu)+2(1-\nu))}{2r^2}$
0
0
$\frac{\nu}{r}$
$\frac{n(3-4\nu)}{2r^2}$
$\frac{n(1-\nu)}{r}$
$\frac{nz(3-4\nu)}{2r^2}$
2+ $\frac{n^2(1-2\nu)}{2}$
$\frac{z(n^2(1-2\nu)+2)}{2r}$
0
0
2ν
$\frac{n(3-2\nu)}{2r}$
n
$\frac{nz(3-2\nu)}{2r}$
$\frac{z^2(n^2(1-2\nu)+2(1-\nu))}{2r^2}$
0
$\frac{(1-2\nu)}{2}$
$\frac{\nu z}{r}$
$\frac{nz(3-4\nu)}{2r^2}$
$\frac{nz(1-\nu)}{r}$
$\frac{nz^2(3-4\nu)}{2r^2}$
+ $\frac{(1-2\nu)}{2}$
$\frac{n^2(1-2\nu)}{2r^2}$
$\frac{n^2(1-2\nu)}{2r}$
$\frac{n^2z(1-2\nu)}{2r^2}$
0
0
$\frac{-n(1-2\nu)}{2r}$
$\frac{(n^2+1)(1-2\nu)}{2}$
$\frac{n^2z(1-2\nu)}{2r}$
0
0
$\frac{-n(1-2\nu)}{2}$
$\frac{n^2z^2(1-2\nu)}{2r^2}$
+(1+ν)
$\frac{n\nu}{r}$
$n\nu$
$\frac{nz(4\nu-1)}{2r}$
$\frac{2n^2(1-\nu)+(1-2\nu)}{2r^2}$
$\frac{n^2(1-\nu)}{r}$
$\frac{z(2n^2(1-\nu)+(1-2\nu))}{2r^2}$
$n^2(1-\nu)$
$\frac{n^2z(1-\nu)}{r}$
$\frac{z^2(2n^2(1-\nu)+(1-2\nu))}{2r^2}$
+ $\frac{(1-2\nu)}{2}$

SYMMETRY

APPENDIX III

Sample Problem of a Heavy Beam with Circular Cross-section Bent by Its Own Weight

A Uranium rod (4" O.D., 16" long) simply supported at both ends is bent by its own weight (as shown in Fig.6-a). The material properties of Uranium metal are assigned as :

$E = 2.8 \times 10^7$	psi	----Young's modulus
$= 0.33$		----Poisson's ratio
$= 0$	in/in.F	----Thermal expansion Coeff.
$= 22.5$	$lbf/in.^3$	----Density

(i) Analytical solution :

Pearson [37] reported an analytical solution to this sample problem. In his work, he solved the governing equilibrium equations :

$$\frac{\partial \sigma^{rr}}{\partial r} + \frac{\partial \sigma^{r\theta}}{r\partial \theta} + \frac{\partial \sigma^{rz}}{\partial z} + \frac{\sigma^{rr} - \sigma^{\theta\theta}}{r} + g\rho\cos\theta = 0$$

$$\frac{\partial \sigma^{r\theta}}{\partial r} + \frac{\partial \sigma^{\theta\theta}}{r\partial \theta} + \frac{\partial \sigma^{z\theta}}{\partial z} + \frac{2\sigma^{r\theta}}{r} - g\rho\sin\theta = 0$$

$$\frac{\partial \sigma^{zr}}{\partial r} + \frac{\partial \sigma^{z\theta}}{r\partial \theta} + \frac{\partial \sigma^{zz}}{\partial z} + \frac{\sigma^{zr}}{r} = 0$$

under the boundary conditions :

(1) Surface traction on rod surface except both end sections vanishes:

$$\sigma_{rr} = 0 \qquad \text{at} \quad r = a$$

$$\sigma_{rz} = 0 \qquad \text{at} \quad r = a$$

$$\sigma_{r\theta} = 0 \qquad \text{at} \quad r = a$$

(2) Vertical shift is symmetry about $z = \ell/2$ at the z-axis :

$$\left(\frac{\partial U^y}{\partial z}\right)_{r=0,z=\ell/2} = 0$$

Where $U^y = -u^r \cos\theta + u^\theta \sin\theta$ ... vertical shift

(3) Longitudinal shift is symmetric about $z = \ell/2$ at the z-axis :

$$u^z = 0 \qquad \text{at} \quad r = 0, \quad z = \ell/2$$

(4) The vertical displacements at the centre of both end sections vanish :

$$U^y = 0 \qquad \text{at} \quad r = 0, \quad z = 0 \quad \text{and} \quad z = \ell$$

(5) The horizontal displecements at the centre of both end sections vanish :

$$U^x = 0 \qquad \text{at} \quad r = 0, \quad z = 0 \quad \text{and} \quad z = \ell$$

Where $U^x = u^r \sin\theta + u^\theta \cos\theta$

(6) The total vertical shear over each of the end sections equals to one half of the total load :

$$\int_0^{2\pi}\int_0^a (-\sigma_{zr}\cos\theta + \sigma_{z\theta}\sin\theta)\,r\,dr\,d\theta = 1/2\,\pi a^2 \ell\rho \text{ at } z=0 \text{ and } z=\ell$$

(7) The total horizontal shear over each of the end sections vanishes :

$$\int_0^{2\pi}\int_0^a (\sigma_{zr} \sin\theta + \sigma_{z\theta}\cos\theta) r dr d\theta = 0 \quad \text{at } z=0 \text{ and } z=\ell$$

(8) The total traction over each of the end sections vanishes :

$$\int_0^{2\pi}\int_0^a \sigma_{zz}\, r dr d\theta = 0 \quad \text{at } z=0 \text{ and } z=\ell$$

(9) The bending moment at each of the end sections vanishes :

$$M_1 = \int_0^{2\pi}\int_0^a \sigma_{zz}\, r \sin\theta\, r dr d\theta = 0 \quad \ldots \text{ horizontal bending moment}$$

$$M_2 = \int_0^{2\pi}\int_0^a \sigma_{zz}\, r \cos\theta\, r dr d\theta = 0 \quad \ldots \text{ vertical bending moment}$$

at $z=0$ and $z=\ell$

The solution of displacement components and σ_{zz} of Pearson's paper may be found in Figure 7, 8, 9, and 10 in comparison with the finite element solution and simple beam solution.

(ii) Finite element method :

The loading situation in this problem is simply the mode 1, i.e. the gravity of the rod, or :

$$\begin{Bmatrix} f^r \\ f^z \\ f^\theta \end{Bmatrix} = \begin{Bmatrix} f_1^r \cdot \cos\theta \\ f_1^z \cdot \cos\theta \\ f_1^\theta \cdot \sin\theta \end{Bmatrix}$$

with $f_1^r = f_1^\theta = \rho g$, and $f_1^z = 0$

No surface traction is employed. The finite element model is shown in Figure 5-b, with the following boundary conditions :

(1') Rod surface except the end sections is free of traction.

(2') Longitudinal displacement is symmetrical about the mid-span :

$$u^z = 0 \qquad \text{at} \quad z = \ell/2$$

(3') Longitudinal displacement (u^z) vanishes at the centre axis. (This is a well-known requirement of Bernoulli's theory in which he assumed the longitudinal displacement to be proportional to the radial distance from the neutral axis for each cross-section; or the famous " plane remains plane " hypothesis.)

(4') u^r and u^θ vanish on terminal cross-sections.

Boundary condition (4') is obviously not consistent with boundary conditions (6), (7), (8), and (9) used in the analytical approach (i). In the finite element approach, only nodal force, nodal displacement and element surface traction components are inputed as boundary conditions; the total shear, total traction and total bending moment on any section of the boundary surface usually are not taken into consideration in forming the stiffness equation. Experience showed that for problems of simply supported beam, the in-plane displacement components on terminal cross-sections are relatively small in comparison with those on the off-ends region (about one thousandth of the value on

the cross-section 0.5" off the end sections). Thus, condition (4') is considered to be reasonable assumption.

It has to be noted that in this analysis, rotation is not taken into consideration as one of the degrees of freedom. It is true that this analysis is valid for small rotation problems only.

(iii) Simple beam theory :

In the simple beam theory, the sample problem is approximated by a simple beam of the same length simply supported at both ends. The weight of the beam is approximated by a uniform load distributed over the whole length and is given by

$$\omega = \rho A = \rho \pi r_o^2$$

in which r_o is the radius of the beam in inches and ρ is the density of the beam material in lbf/in.^{3}

Solution to the above simple beam problem is available in many stress analysis handbooks. Solutions of deflection (or sagging) δ and bending stress σ_b can be written as [38] :

$$\delta = \frac{-1}{24}\frac{\omega z}{EI}(\ell^3 - 2\ell z^2 + z^3)$$

$$\delta_{max} = \frac{-5}{384}\frac{w\ell^3}{EI} \qquad \text{at} \quad z = \ell/2$$

$$\sigma_b = \frac{Mr}{I} = \frac{r}{I}w\left(\frac{z}{2} - \frac{z^2}{2}\right)$$

and $$(\sigma_b)_{max} = \frac{r}{I} w \frac{\ell}{8} \quad , \qquad \text{at} \quad z = \ell/2$$

In which w = total weight of the beam = $\omega \ell = \rho \pi r_o^2 \ell$

E = Young's modulus of beam material

I = moment of inertia of the beam cross-section

M = bending moment at various position

$= w \left(\frac{z}{2} - \frac{z^2}{2\ell} \right)$

APPENDIX IV
INTEGRANDS OF THE MODE-MIXING STIFFNESS MATRIX
(MODE ZERO AND MODE ONE ONLY)

NOTE :

(I) BECAUSE OF SYMMETRY, ONLY THE UPPER TRIANGULAR PART OF THE MATRIX IS PRINTED

(II)
```
A=COS(θ)
B=SIN(θ)
```

(III)
```
XI(1)=1.
XI(2)=1/R
XI(3)=1/R**2
XI(4)=Z/R
XI(5)=Z/R**2
XI(6)=Z**2/R**2
```

(IV) DS(I,J) FOR I,J=1,2,3,4,5,6 ARE THE ELASTO-PLASTIC MATRIX, $[C^{ep}]$, AS SHOWN IN EQ.(2-4-30) IN CHAPTER II.

1ST ROW ELEMENTS

```
101 FCT=DS(3,3)*XI(3)
102 FCT=(DS(3,1)+DS(3,3))*XI(2)
103 FCT=DS(3,3)*XI(5)+DS(3,4)*XI(2)
104 FCT=0.0
105 FCT=DS(3,4)*XI(2)
106 FCT=DS(3,2)*XI(2)
107 FCT=-DS(3,5)*XI(3)
108 FCT=0.0
109 FCT=-DS(3,5)*XI(5)+DS(3,6)*XI(2)
110 FCT=DS(3,3)*XI(3)*A-DS(3,5)*XI(3)*B
111 FCT=(DS(3,1)+DS(3,3))*XI(2)*A-DS(3,5)*XI(2)*B
112 FCT=DS(3,3)*XI(5)*A+DS(3,4)*XI(2)*A-DS(3,5)*XI(5)*B
113 FCT=-DS(3,6)*XI(3)*B
114 FCT=DS(3,4)*XI(2)*A-DS(3,6)*XI(2)*B
115 FCT=DS(3,2)*XI(2)*A-DS(3,6)*XI(5)*B
116 FCT=DS(3,3)*XI(3)*A-DS(3,5)*XI(3)*B
117 FCT=DS(3,3)*XI(2)*A
118 FCT=DS(3,3)*XI(5)*A-DS(3,5)*XI(5)*B+DS(3,6)*XI(2)*B
```

2ND ROW ELEMENTS

```
202 FCT=(DS(1,1)+DS(1,3)+DS(3,1)+DS(3,3))*XI(1)
203 FCT=(DS(1,3)+DS(3,3))*XI(4)+(DS(1,4)+DS(3,4))*XI(1)
204 FCT=0.0
205 FCT=(DS(1,4)+DS(3,4))*XI(1)
206 FCT=(DS(1,2)+DS(3,2))*XI(1)
```

```
207 FCT=-DS(1,5)*XI(2)-DS(3,5)*XI(2)
208 FCT=0.0
209 FCT=-(DS(1,5)+DS(3,5))*XI(4)+(DS(1,6)+DS(3,6))*XI(1)
210 FCT=(DS(1,3)+DS(3,3))*XI(2)*A-(DS(1,5)+DS(3,5))*XI(2)*B
211 FCT=((DS(1,1)+DS(1,3)+DS(3,1)+DS(3,3))*A-(DS(3,5)+DS(1,5))*B)*XI(1
    1)
212 FCT=(DS(1,3)+DS(3,3))*XI(4)*A+(DS(1,4)+DS(3,4))*A*XI(1)-(DS(1,5)+D
    1S(3,5))*XI(4)*B
213 FCT=-(DS(1,6)+DS(3,6))*XI(2)*B
214 FCT=((DS(1,4)+DS(3,4))*A-(DS(1,6)+DS(3,6))*B)*XI(1)
215 FCT=(DS(1,2)+DS(3,2))*A*XI(1)-(DS(1,6)+DS(3,6))*XI(4)*B
216 FCT=(DS(1,3)+DS(3,3))*XI(2)*A-(DS(1,5)+DS(3,5))*XI(2)*B
217 FCT=(DS(1,3)+DS(3,3))*A*XI(1)
218 FCT=(DS(1,3)+DS(3,3))*XI(4)*A-(DS(1,5)+DS(3,5))*XI(4)*B+(DS(1,6)+D
    1S(3,6))*B*XI(1)

        3RD ROW ELEMENTS

303 FCT=DS(3,3)*XI(6)+DS(3,4)*XI(4)+DS(4,3)*XI(4)+DS(4,4)*XI(1)
304 FCT=0.0
305 FCT=DS(3,4)*XI(4)+DS(4,4)*XI(1)
306 FCT=DS(3,2)*XI(4)+DS(4,2)*XI(1)
307 FCT=-DS(3,5)*XI(5)-DS(4,5)*XI(2)
308 FCT=0.0
309 FCT=-DS(3,5)*XI(6)+DS(3,6)*XI(4)-DS(4,5)*XI(4)+DS(4,6)*XI(1)
310 FCT=(DS(3,3)*A-DS(3,5)*B)*XI(5)+(DS(4,3)*A-DS(4,5)*B)*XI(2)
311 FCT=(DS(3,1)*A+DS(3,3)*A-DS(3,5)*B)*XI(4)+(DS(4,1)*A+DS(4,3)*A-DS(
    14,5)*B)*XI(1)
312 FCT=DS(3,3)*XI(6)*A+DS(3,4)*XI(4)*A-DS(3,5)*XI(6)*B+DS(4,3)*XI(4)*
    1A+DS(4,4)*A*XI(1)-DS(4,5)*XI(4)*B
313 FCT=-DS(3,6)*XI(5)*B-DS(4,6)*XI(2)*B
314 FCT=(DS(3,4)*A-DS(3,6)*B)*XI(4)+(DS(4,4)*A-DS(4,6)*B)*XI(1)
315 FCT=DS(3,2)*XI(4)*A-DS(3,6)*XI(6)*B+DS(4,2)*A*XI(1)-DS(4,6)*XI(4)*
    1B
316 FCT=(DS(3,3)*A-DS(3,5)*B)*XI(5)+(DS(4,3)*A-DS(4,5)*B)*XI(2)
317 FCT=DS(3,3)*XI(4)*A+DS(4,3)*A*XI(1)
318 FCT=(DS(3,3)*A-DS(3,5)*B)*XI(6)+DS(3,6)*XI(4)*B+(DS(4,3)*A-DS(4,5)
    1*B)*XI(4)+DS(4,6)*XI(1)*B

        4TH ROW ELEMENTS

400 FCT=0.0
  .
  .
  .
418 FCT=0.0

        5TH ROW ELEMENTS

505 FCT=DS(4,4)*XI(1)
506 FCT=DS(4,2)*XI(1)
507 FCT=-DS(4,5)*XI(2)
508 FCT=0.0
509 FCT=-DS(4,5)*XI(4)+DS(4,6)*XI(1)
```

```
510 FCT=(DS(4,3)*A-DS(4,5)*B)*XI(2)
511 FCT=(DS(4,1)*A+DS(4,3)*A-DS(4,5)*B)*XI(1)
512 FCT=(DS(4,3)*A-DS(4,5)*B)*XI(4)+DS(4,4)*XI(1)*A
513 FCT=-DS(4,6)*XI(2)*B
514 FCT=(DS(4,4)*A-DS(4,6)*B)*XI(1)
515 FCT=DS(4,2)*A*XI(1)-DS(4,6)*XI(4)*B
516 FCT=(DS(4,3)*A-DS(4,5)*B)*XI(2)
517 FCT=DS(4,3)*XI(1)*A
518 FCT=(DS(4,3)*A-DS(4,5)*B)*XI(4)+DS(4,6)*XI(1)*B

        6TH ROW ELEMENTS

606 FCT=DS(2,2)*XI(1)
607 FCT=-DS(2,5)*XI(2)
608 FCT=0.0
609 FCT=-DS(2,5)*XI(4)+DS(2,6)*XI(1)
610 FCT=(DS(2,3)*A-DS(2,5)*B)*XI(2)
611 FCT=(DS(2,1)*A+DS(2,3)*A-DS(2,5)*B)*XI(1)
612 FCT=(DS(2,3)*A-DS(2,5)*B)*XI(4)+DS(2,4)*A*XI(1)
613 FCT=-DS(2,6)*B*XI(2)
614 FCT=(DS(2,4)*A-DS(2,6)*B)*XI(1)
615 FCT=DS(2,2)*A*XI(1)-DS(2,6)*B*XI(4)
616 FCT=(DS(2,3)*A-DS(2,5)*B)*XI(2)
617 FCT=DS(2,3)*A*XI(1)
618 FCT=(DS(2,3)*A-DS(2,5)*B)*XI(4)+DS(2,6)*B*XI(1)

        7TH ROW ELEMENTS

707 FCT=DS(5,5)*XI(3)
708 FCT=0.0
709 FCT=DS(5,5)*XI(5)-DS(5,6)*XI(2)
710 FCT=(DS(5,5)*B-DS(5,3)*A)*XI(3)
711 FCT=(DS(5,5)*B-DS(5,1)*A-DS(5,3)*A)*XI(2)
712 FCT=-(DS(5,3)*A+DS(5,5)*B)*XI(5)-DS(5,4)*A*XI(2)
713 FCT=DS(5,6)*B*XI(3)
714 FCT=(DS(5,6)*B-DS(5,4)*A)*XI(2)
715 FCT=DS(5,6)*B*XI(5)-DS(5,2)*A*XI(2)
716 FCT=(DS(5,5)*B-DS(5,3)*A)*XI(3)
717 FCT=-DS(5,3)*A*XI(2)
718 FCT=(DS(5,5)*B-DS(5,3)*A)*XI(5)-DS(5,6)*B*XI(2)

        8TH ROW ELEMENTS

800 FCT=0.0
  .
  .
  .
818 FCT=0.0

        9TH ROW ELEMENTS

909 FCT=DS(5,5)*XI(6)-(DS(5,6)+DS(6,5))*XI(4)+DS(6,6)*XI(1)
910 FCT=(-DS(5,3)*A+DS(5,5)*B)*XI(5)+(DS(6,3)*A-DS(6,5)*B)*XI(2)
```

```
 911 FCT=-(DS(5,1)*A+DS(5,3)*A-DS(5,5)*B)*XI(4)+(DS(6,1)*A+DS(6,3)*A-DS
    1(6,5)*B)*XI(1)
 912 FCT=-(DS(5,3)*A-DS(5,5)*B)*XI(6)+(DS(6,3)*A-DS(6,5)*B-DS(5,4)*A)*X
    1I(4)+DS(6,4)*A*XI(1)
 913 FCT=DS(5,6)*B*XI(5)-DS(6,6)*B*XI(2)
 914 FCT=-(DS(5,4)*A-DS(5,6)*B)*XI(4)+(DS(6,4)*A-DS(6,6)*B)*XI(1)
 915 FCT=DS(5,6)*B*XI(6)-(DS(5,2)*A+DS(6,6)*B)*XI(4)+DS(6,2)*A*XI(1)
 916 FCT=(-DS(5,3)*A+DS(5,5)*B)*XI(5)+(DS(6,3)*A-DS(6,5)*B)*XI(2)
 917 FCT=-DS(5,3)*A*XI(4)+DS(6,3)*A*XI(1)
 918 FCT=(DS(5,5)*B-DS(5,3)*A)*XI(6)+(DS(6,3)*A-DS(6,5)*B-DS(5,6)*B)*XI
    1(4)+DS(6,6)*B*XI(1)

        10TH ROW ELEMENTS

1010 FCT=(DS(3,3)*A-DS(3,5)*B)*A*XI(3)-(DS(5,3)*A-DS(5,5)*B)*B*XI(3)
1011 FCT=(DS(3,1)*A+DS(3,3)*A-DS(3,5)*B)*A*XI(2)-(DS(5,1)*A+DS(5,3)*A-I
    1S(5,5)*B)*B*XI(2)
1012 FCT=(DS(3,3)*A**2-DS(3,5)*A*B-DS(5,3)*A*B+DS(5,5)*B**2)*XI(5)+(DS
    13,4)*A-DS(5,4)*B)*A*XI(2)
1013 FCT=(DS(5,6)*B-DS(3,6)*A)*B*XI(3)
1014 FCT=(DS(3,4)*A**2-DS(3,6)*A*B-DS(5,4)*A*B+DS(5,6)*B**2)*XI(2)
1015 FCT=(DS(5,6)*B-DS(3,6)*A)*B*XI(5)+(DS(3,2)*A-DS(5,2)*B)*A*XI(2)
1016 FCT=(DS(3,3)*A**2-DS(3,5)*A*B-DS(5,3)*A*B+DS(5,5)*B**2)*XI(3)
1017 FCT=(DS(3,3)*A-DS(5,3)*B)*A*XI(2)
1018 FCT=(DS(3,3)*A**2-DS(3,5)*A*B-DS(5,3)*A*B+DS(5,5)*B**2)*XI(5)+(DS
    13,6)*A-DS(5,6)*B)*B*XI(2)

        11TH ROW ELEMENTS

1111 FCT=(((DS(1,1)+DS(1,3)+DS(3,1))*A-(DS(1,5)+DS(3,5))*B)*A-(DS(5,1)
    1A+DS(5,3)*A-DS(5,5)*B)*B)*XI(1)
1112 FCT=((DS(1,3)+DS(3,3))*A**2-(DS(1,5)+DS(3,5))*A*B+DS(5,5)*B**2-DS
    15,3)*A*B)*XI(4)+((DS(1,4)+DS(3,4))*A-DS(5,4)*B)*A*XI(1)
1113 FCT=(DS(5,6)*B**2-(DS(1,6)+DS(3,6))*A*B)*XI(2)
1114 FCT=((DS(1,4)*A-DS(1,6)*B+DS(3,4)*A-DS(3,6)*B)*A-(DS(5,4)*A-DS(5,
    1)*B)*B)*XI(1)
1115 FCT=((DS(1,2)+DS(3,2))*A-DS(5,2)*B)*A*XI(1)+(DS(5,6)*B-(DS(1,6)+D
    1(3,6))*A)*B*XI(4)
1116 FCT=((DS(1,3)*A-DS(1,5)*B+DS(3,3)*A-DS(3,5)*B)*A-(DS(5,3)*A-DS(5,
    1)*B)*B)*XI(2)
1117 FCT=((DS(1,3)+DS(3,3))*A-DS(5,3)*B)*A*XI(1)
1118 FCT=((DS(1,3)+DS(3,3))*A**2-(DS(1,5)+DS(3,5)+DS(5,3))*A*B+DS(5,5)
    1B**2)*XI(4)+((DS(1,6)+DS(3,6))*A-DS(5,6)*B)*B*XI(1)

        12TH ROW ELEMENTS

1212 FCT=(DS(3,3)*A**2-DS(3,5)*A*B-DS(5,3)*A*B+DS(5,5)*B**2)*XI(6)+(DS
    13,4)*A**2-DS(5,4)*A*B+DS(4,3)*A**2-DS(4,5)*A*B)*XI(4)+DS(4,4)*A**
    2*XI(1)
1213 FCT=(DS(5,6)*B-DS(3,6)*A)*B*XI(5)-DS(4,6)*A*B*XI(2)
1214 FCT=(DS(3,4)*A**2-DS(3,6)*A*B-DS(5,4)*A*B+DS(5,6)*B**2)*XI(4)+(DS
    14,4)*A-DS(4,6)*B)*A*XI(1)
1215 FCT=(DS(5,6)*B-DS(3,6)*A)*B*XI(6)+(DS(3,2)*A-DS(4,6)*B-DS(5,2)*B)
```

```
     1A*XI(4)+DS(4,2)*A**2*XI(1)
 1216 FCT=(DS(3,3)*A**2-DS(3,5)*A*B-DS(5,3)*A*B+DS(5,5)*B**2)*XI(5)+(DS(
     14,3)*A-DS(4,5)*B)*A*XI(2)
 1217 FCT=(DS(3,3)*A-DS(5,3)*B)*A*XI(4)+DS(4,3)*A**2*XI(1)
 1218 FCT=(DS(3,3)*A**2-DS(3,5)*A*B-DS(5,3)*A*B+DS(5,5)*B**2)*XI(6)+(DS(
     13,6)*A*B-DS(5,6)*B**2+DS(4,3)*A**2-DS(4,5)*A*B)*XI(4)+DS(4,6)*A*B*
     2XI(1)

          13TH ROW ELEMENTS

 1313 FCT=DS(6,6)*B**2*XI(3)
 1314 FCT=(DS(6,6)*B-DS(6,4)*A)*B*XI(2)
 1315 FCT=(DS(6,6)*B*XI(5)-DS(6,2)*A*XI(2))*B
 1316 FCT=(DS(6,5)*B-DS(6,3)*A)*B*XI(3)
 1317 FCT=-DS(6,3)*A*B*XI(2)
 1318 FCT=-(DS(6,3)*A-DS(6,5)*B)*XI(5)*B-DS(6,6)*B**2*XI(2)

          14TH ROW ELEMENTS

 1414 FCT=(DS(4,4)*A**2-DS(4,6)*A*B-DS(6,4)*A*B+DS(6,6)*B**2)*XI(1)
 1415 FCT=(DS(4,2)*A-DS(6,2)*B)*A*XI(1)+(DS(6,6)*B-DS(4,6)*A)*B*XI(4)
 1416 FCT=(DS(4,3)*A**2-DS(4,5)*A*B-DS(6,3)*A*B-DS(6,5)*B**2)*XI(2)
 1417 FCT=(DS(4,3)*A-DS(6,3)*B)*A*XI(1)
 1418 FCT=(DS(4,3)*A**2-DS(4,5)*A*B-DS(6,3)*A*B+DS(6,5)*B**2)*XI(4)+(DS(
     14,6)*A-DS(6,6)*B)*B*XI(1)

          15TH ROW ELEMENTS

 1515 FCT=DS(2,2)*A**2*XI(1)-(DS(2,6)+DS(6,2))*A*B*XI(4)+DS(6,6)*B**2*XI
     1(6)
 1516 FCT=(DS(2,3)*A-DS(2,5)*B)*A*XI(2)-(DS(6,3)*A-DS(6,5)*B)*B*XI(5)
 1517 FCT=DS(2,3)*A**2*XI(1)-DS(6,3)*A*B*XI(4)
 1518 FCT=(DS(2,3)*A**2-DS(2,5)*B*A-DS(6,6)*B**2)*XI(4)+DS(2,6)*A*B*XI(1
     1)+(DS(6,5)*B-DS(6,3)*A)*B*XI(6)

          16TH ROW ELEMENTS

 1616 FCT=(DS(3,3)*A**2-DS(3,5)*A*B-DS(5,3)*A*B+DS(5,5)*B**2)*XI(3)
 1617 FCT=(DS(3,3)*A**2-DS(5,3)*A*B)*XI(2)
 1618 FCT=(DS(3,3)*A**2-DS(3,5)*A*B-DS(5,3)*A*B+DS(5,5)*B**2)*XI(5)+(DS(
     13,6)*A-DS(5,6)*B)*B*XI(2)

          17TH ROW ELEMENTS

 1717 FCT=DS(3,3)*A**2*XI(1)
 1718 FCT=(DS(3,3)*A**2-DS(3,5)*A*B)*XI(4)+DS(3,6)*A*B*XI(1)

          18TH ROW ELEMENT

 1800 FCT=(DS(3,3)*A**2-DS(3,5)*A*B-DS(5,3)*A*B+DS(5,5)*B**2)*XI(6)+(DS(
     13,6)*A*B-DS(5,6)*B**2+DS(6,3)*A*B-DS(6,5)*B**2)*XI(4)+DS(6,6)*B**2
     2*XI(1)
```

TABLE 1

	NLSTRS		PEARSON'S SOLU.		SIMPLE BEAM THEORY	
ρ $\frac{lbf}{in^3}$	δ 10^{-3} in	σ_b psi	δ 10^{-3} in	σ_b psi	δ 10^{-3}in	σ_b psi
22.5	0.739	1273	0.742	1263	0.686	1260
50.0	1.642	2829	1.650	2808	1.370	2520
100.0	3.284	5658	3.300	5615	2.740	5040

Comparison of the sagging and bending stress solutions of the sample problem in Appendix III for three tube materials of different densities (δ is the sagging at point A and δ_b is the bending stress at point B of Figure 6.)

TABLE 2

	NTEPSA		NLSTRS		SIMPLE BEAM THEORY	
ρ $\frac{lbf}{in^3}$	δ 10^{-3} in	σ_b psi	δ 10^{-3} in	σ_b psi	δ 10^{-3} in	σ_b psi
22.5	0.531	790	0.531	790	0.439	806
50.0	1.180	1750	1.179	1750	0.880	1613
100.	2.359	3500	2.358	3500	1.760	3226

Comparison of the sagging and bending stress solutions of the sample problem in Chapter V, 5.2 (i) for three tube materials of different densities (δ is the sagging at point A and δ_b is the binding stress at point B of Figure 11.)

TABLE 3

	NTEPSA			TEPSA		
ρ ksi	ε^{zz} 10^{-2} in/in	σ^{zz} ksi	u^r 10^{-3} in	ε^{zz} 10^{-2} in/in	σ^{zz} ksi	u^r 10^{-3} in
20.0	0.1*	20.0	0.4716	0.07	20.0	0.4716
35.0	0.1	35.0	1.0608	0.14	35.0	1.0619
39.5	0.3	39.5	2.1482	0.27	39.5	2.1862
40.0	0.4	40.0	4.0000	0.47	40.0	4.2408
40.5	1.0	40.4	9.3237	1.05	40.4	10.067
41.7	2.4	41.4	23.906	2.67	41.6	26.239
43.2	4.3	42.7	42.69	4.78	43.0	47.28

Comparison of the axial strain, stress and radial displacement solutions of the sample problem in Chapter V, 5.2 (ii) (ε^{zz} and σ^{zz} is respectively the axial strain, axial stress at point B and u^r is the radial displacement at point A of Figure 11).

TABLE 4

	NLSTRS	3-Dimension F.E.
Total nodes	18	162
Total elements	8	72
Stiffness matrix size	54 x 54	486 x 486
Total 10. Integration points	23,328	2,239,488

Comparison of computing Effort between NLSTRS code and an equivalent 3-D elasticity F.E. program.

TABLE 5

	NTEPSA-2 mode	3-Dimension F.E.
Total nodes	18	162
Total elements	8	72
Stiffness matrix size	108 x 108	486 x 486
Integration points	839,808	2,239,188

Comparison of computing effort between NTEPSA code and an equivalent 3-D thermal elasto-plastic F.E. program.

TABLE 6

	Combined F.E. and Fourier expansion	3-D F.E.
Total nodes	18	162
Total elements	8	72
Stiffness matrix size	162 x 162	485 x 486
Integration points	3,359,232	2,239,488

TABLE 7

MODEL	4 element		8 element		16 element	
P(ksi)	$\bar{\varepsilon}$(%)	$\delta(10^{-3}$ in)	$\bar{\varepsilon}$(%)	$\delta(10^{-3}$ in)	$\bar{\varepsilon}$(%)	$\delta(10^{-3}$ in)
0	0.002	0.486	0.002	0.531	0.002	0.533
39	0.201	2.149	0.204	3.705	0.203	3.621
39.8	0.273	2.790	0.312	7.482	0.307	6.986
40.7	0.465	3.176	1.14	9.747	0.988	8.923
41.7	0.796	3.311	2.22	10.58	2.02	9.856
43.2	1.026	3.394	3.94	11.31	3.79	10.86

Solutions of sagging at Point A (see Fig. 11) obtained by "NTEPSA" code for three different finite element discretizations at various loading stages.

TABLE 8

	I_1	I_2	I_3
7	2.8560	0.2717×10^{-1}	3.5410
9	2.8492	0.8879×10^{-3}	3.4921
12	2.8490	0.4361×10^{-3}	3.5043
16	2.8488	-0.1002×10^{-4}	3.5040
24	2.8488	0.4422×10^{-5}	3.5040
32	2.8488	0.2499×10^{-5}	3.5040

Integration results of I_1, I_2, I_3 by gaussian quadrature scheme with 7, 9, 12, 16, 24, 32 integration points.

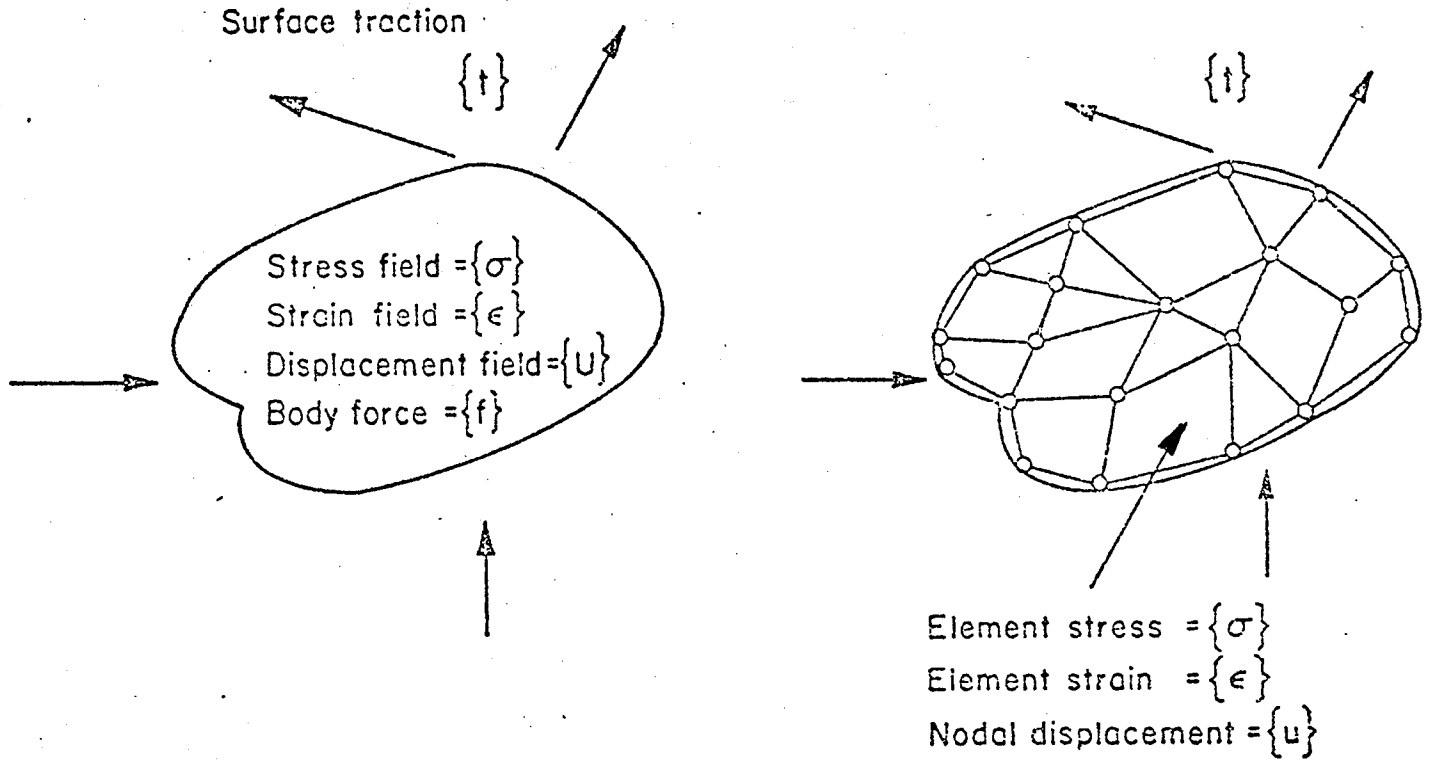

Figure 1 Discretization of a Solid Body

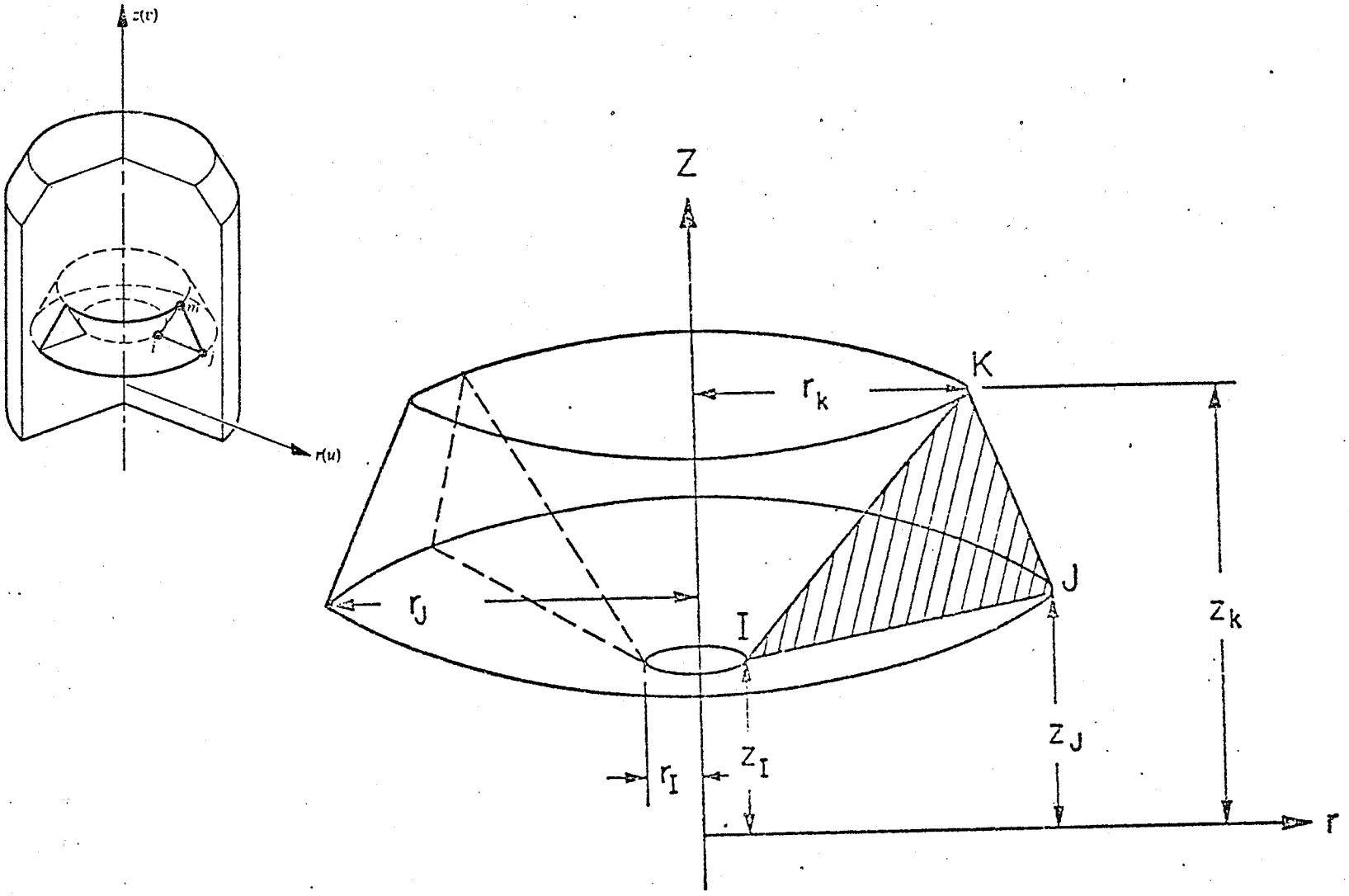

Figure 2 Finite Element Idealization of an Axisymmetric Solid

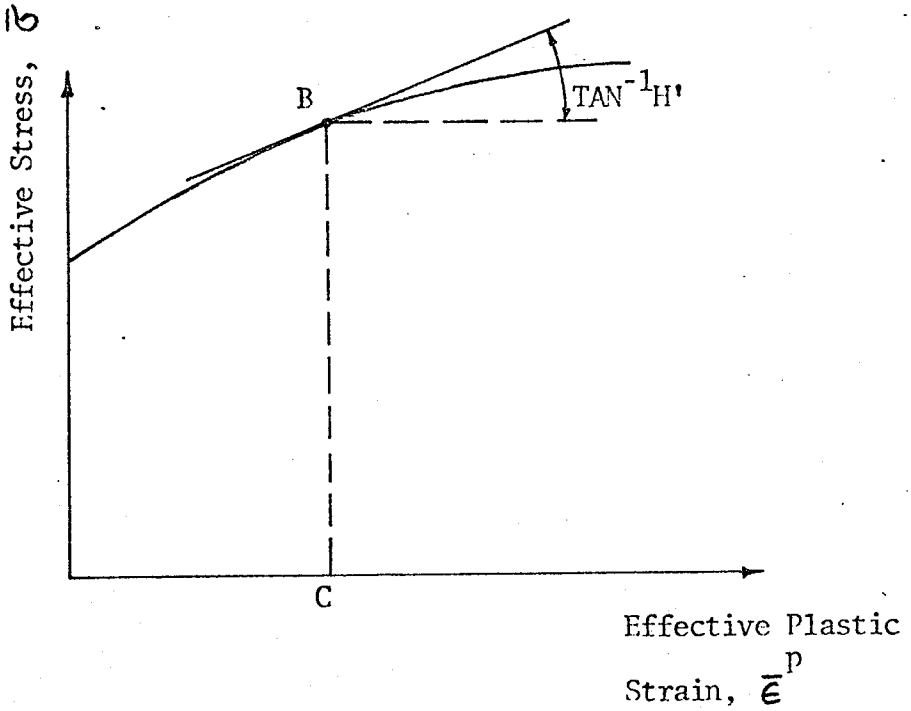

Fig. 3 Effective Stress - Effective Plastic Strain Curve

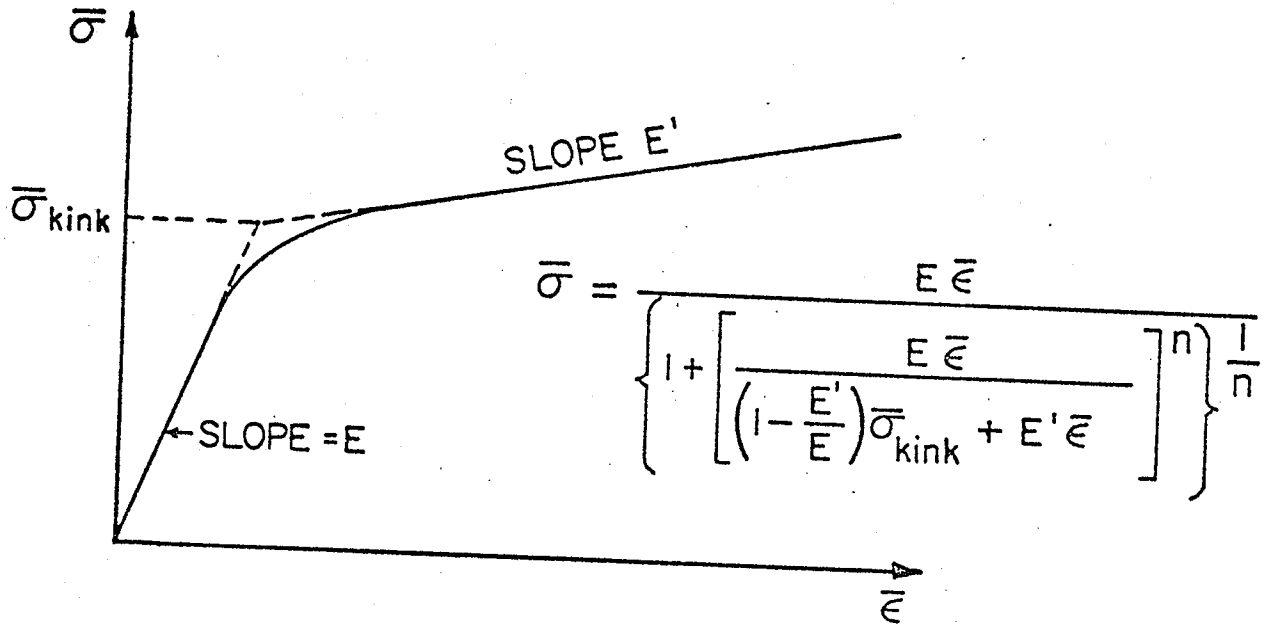

Figure 4 Polynomial Approximation of Stress-Strain Relations

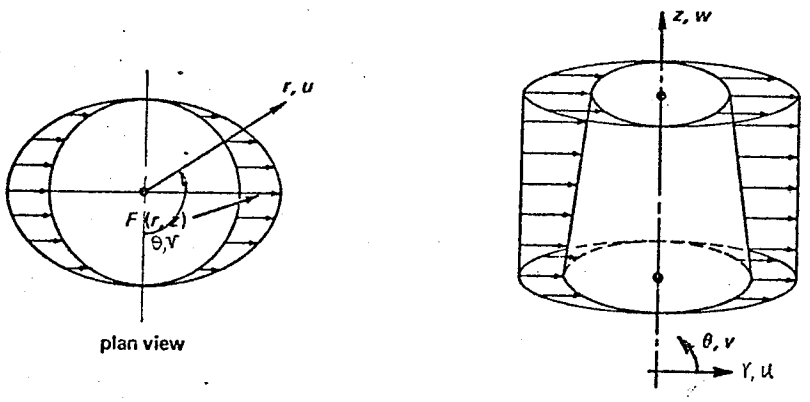

(a)

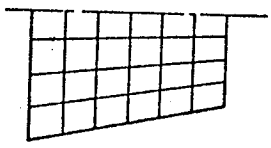

(b)

Fig. 5 (a) An Axisymmetric Solid Subject to Non-axisymmetric Loads

(b) Finite Element Discretization of The Solid

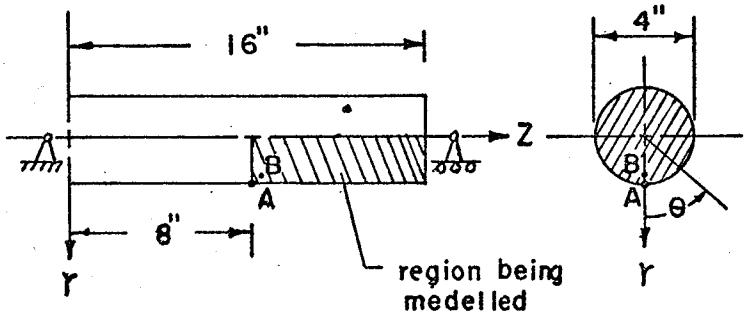

(a)

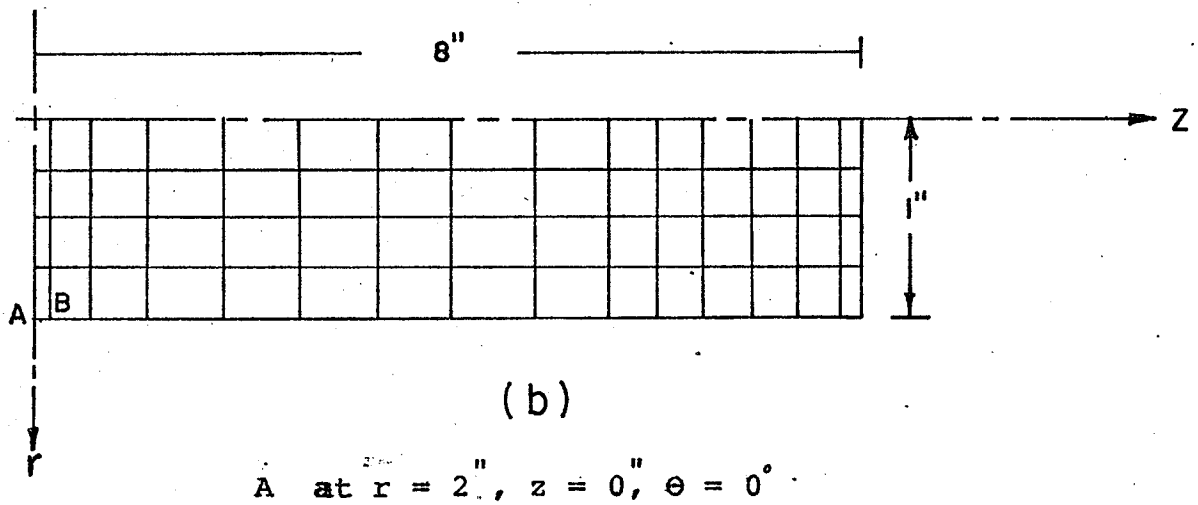

(b)

A at $r = 2''$, $z = 0''$, $\theta = 0°$

B at $r = 1.75''$, $z = 0.1''$, $\theta = 0°$

Figure 6 (a) A Simply Supported Beam Bent by Its Own Weight

(b) Finite Element Discretization of One Quarter Region of The Beam

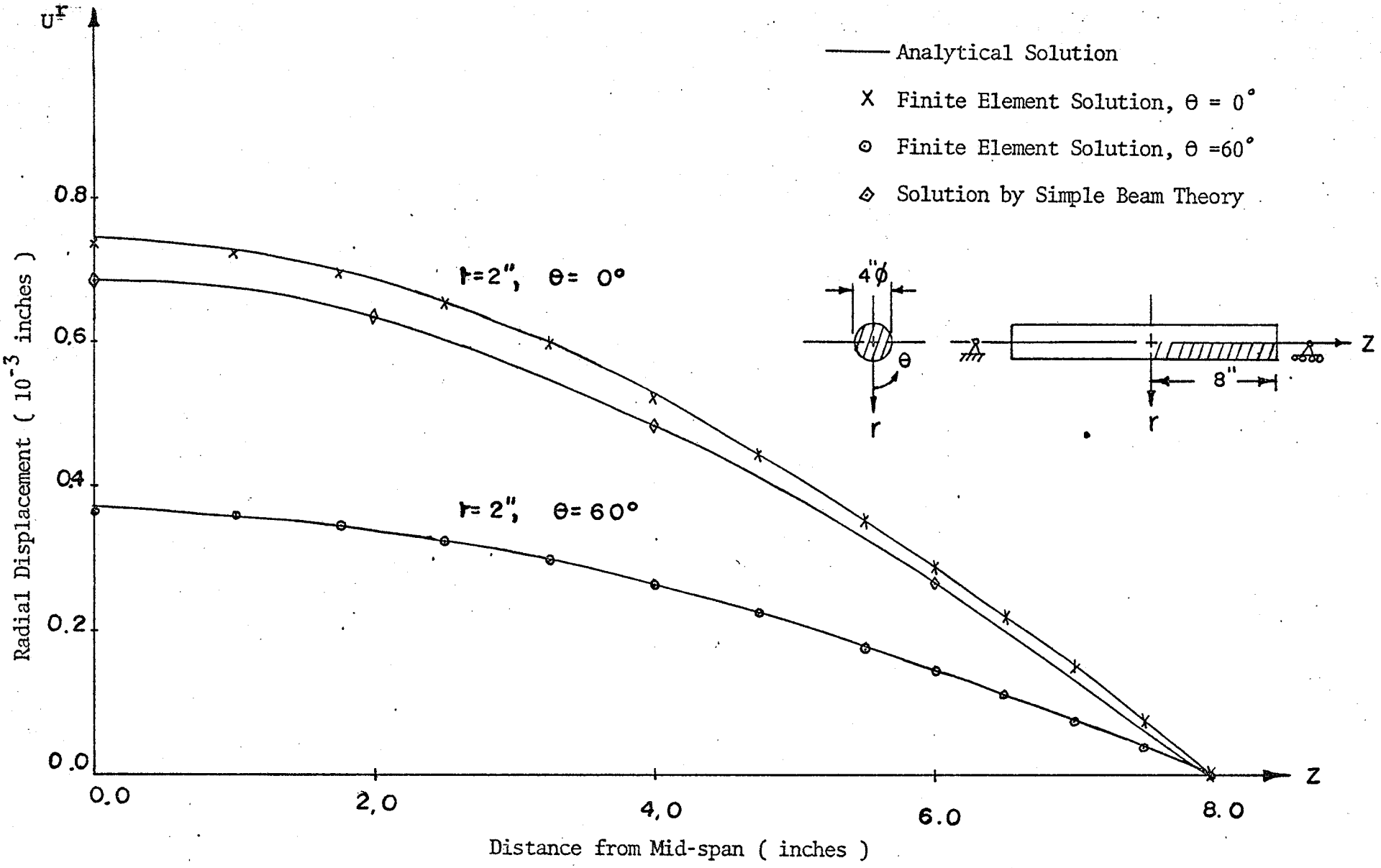

Figure 7 Radial Displacement v.s. Logitudinal Distance from Mid-span

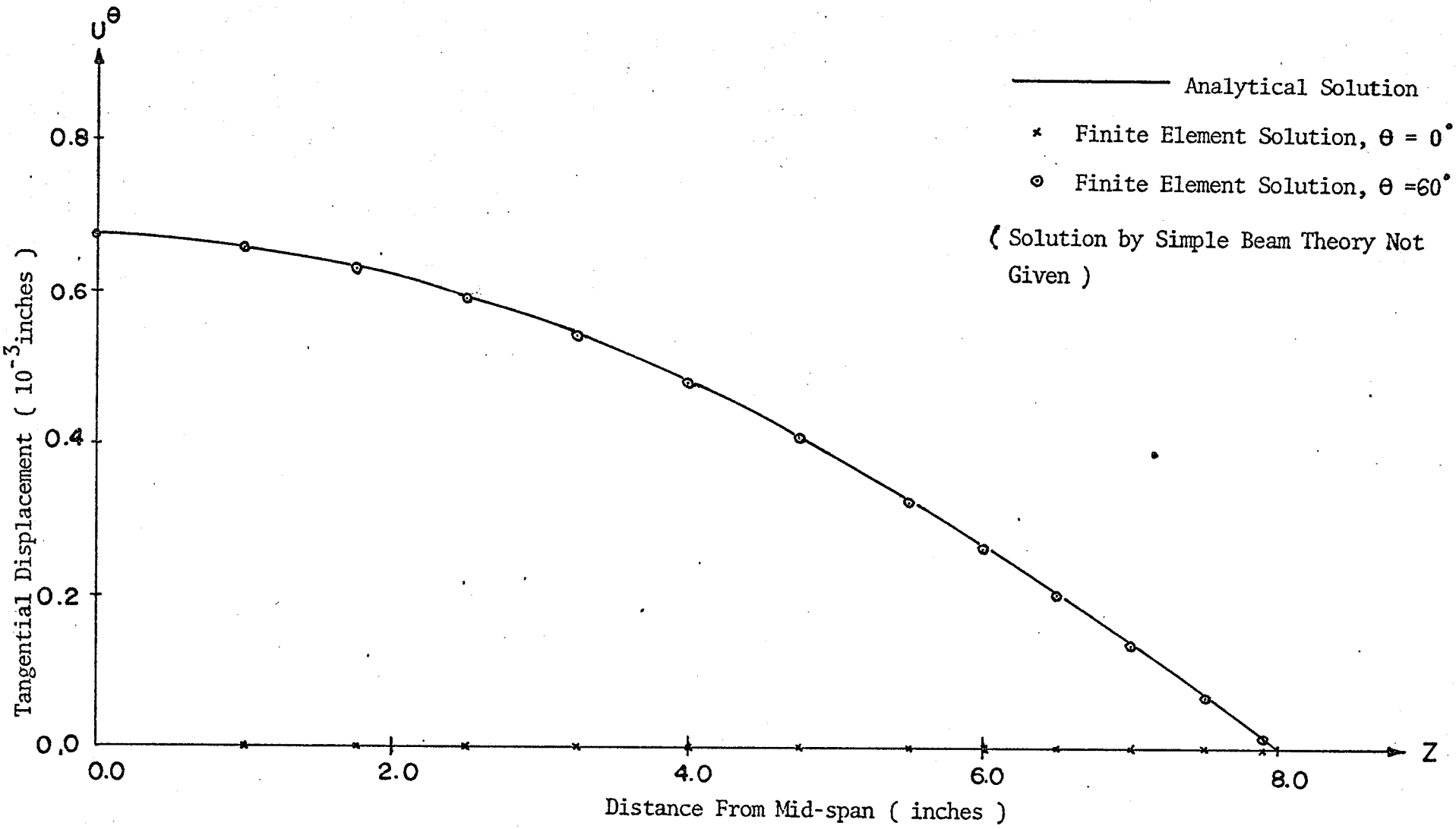

Figure 8 Tangential Displacement v.s. Longitudinal Distance from Mid-span

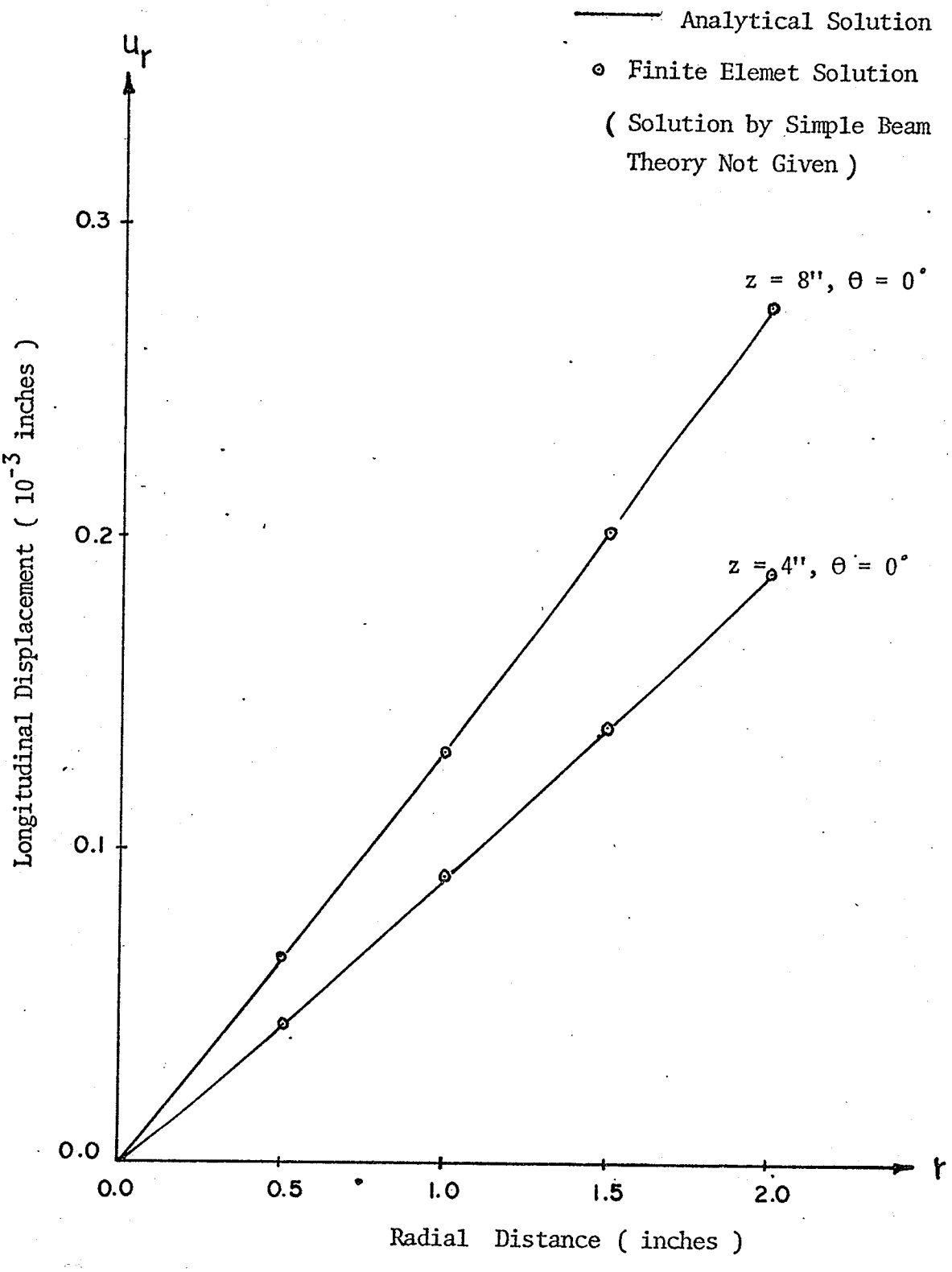

Figure 9 Logitudinal Displacement v.s. Radial Distance from Center Axis (at quarter-span and end section)

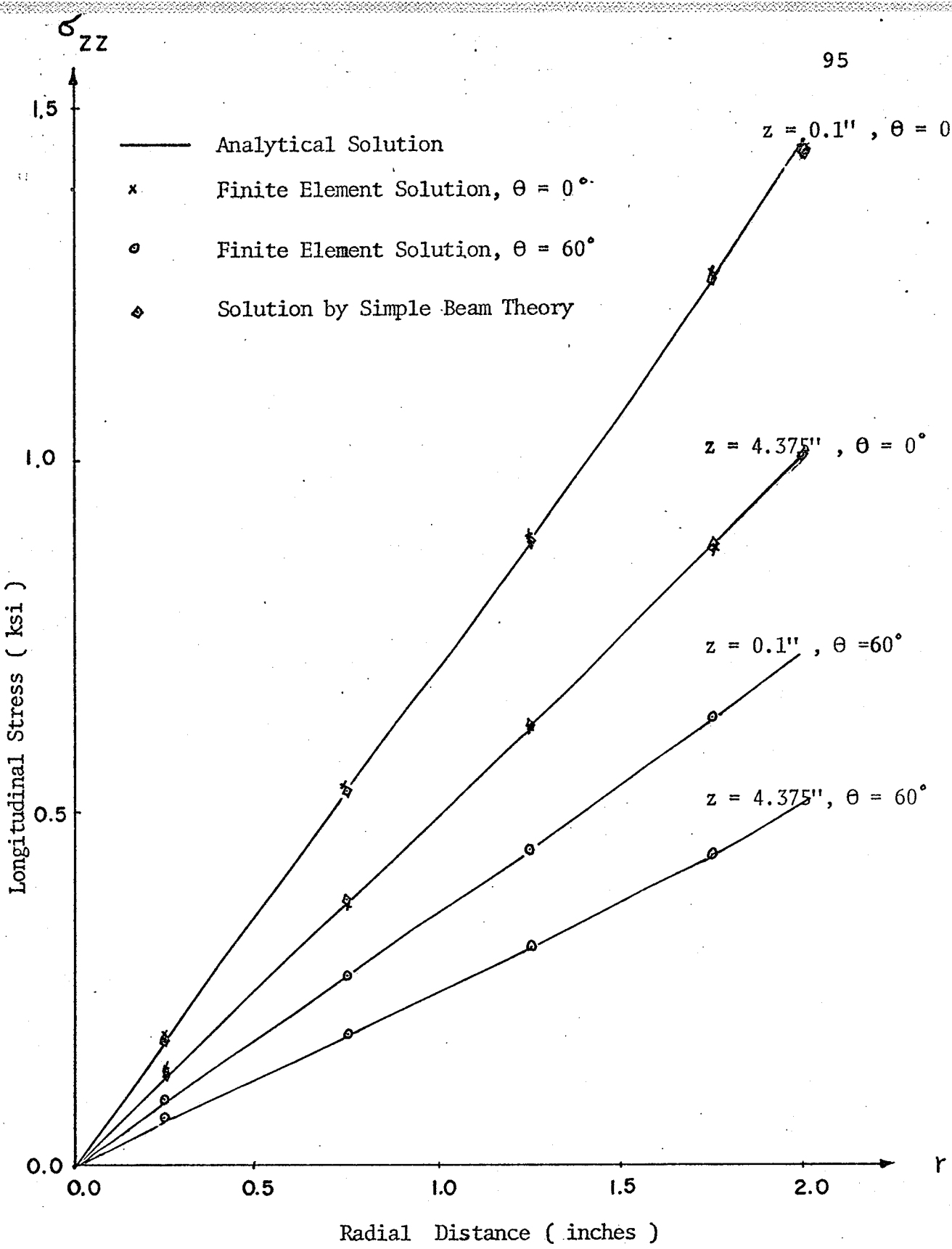

Figure 10 Longitudinal Stress, σ_{zz} , v.s. Radinal Distance from Center Axis (at cross-sections near mid-span and quarter span)

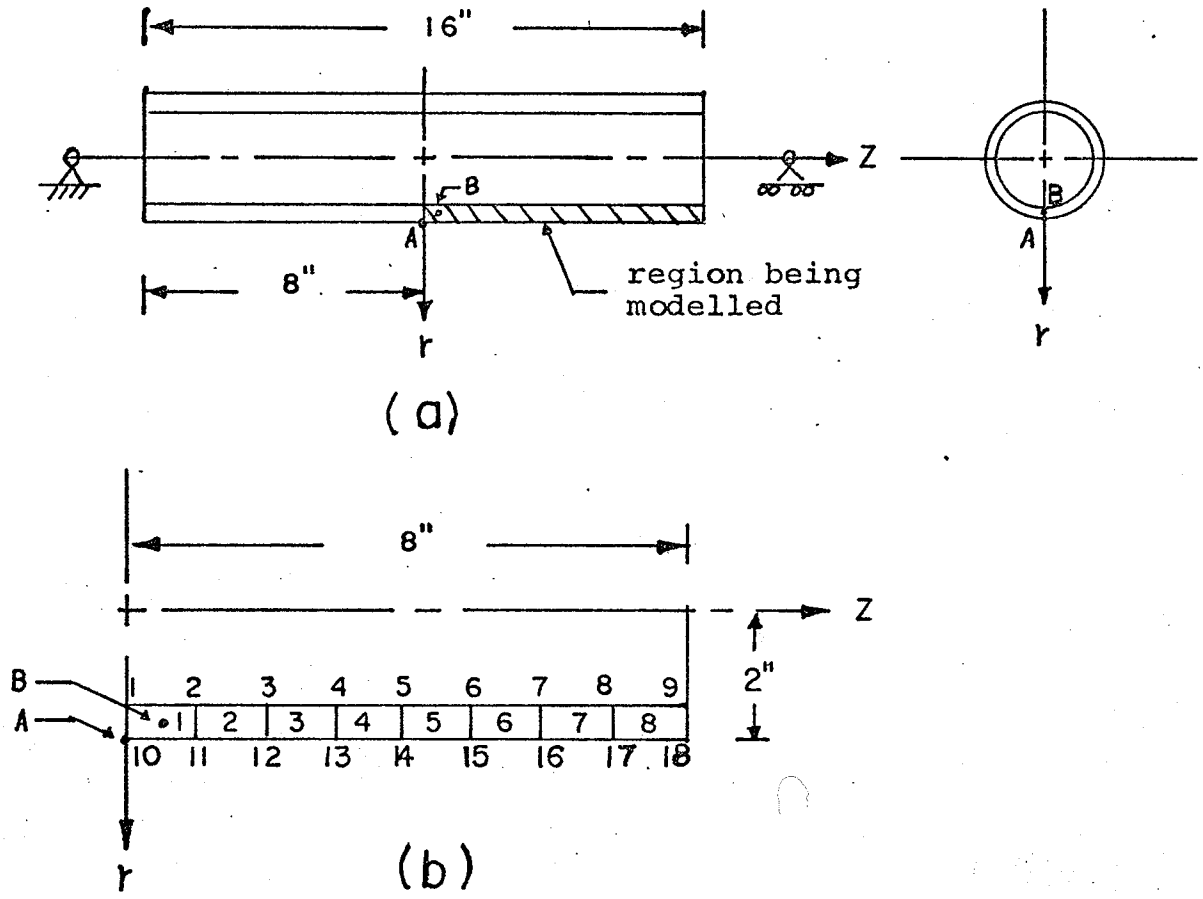

A at r=2", z=0", θ=0°

B at r=1.75", z=0", θ=0°

Figure 11 (a) A Simply Supported Tube Bent by Its Own Weight

(b) Finite Elemet Discretization of One Quarter Region of The Tube

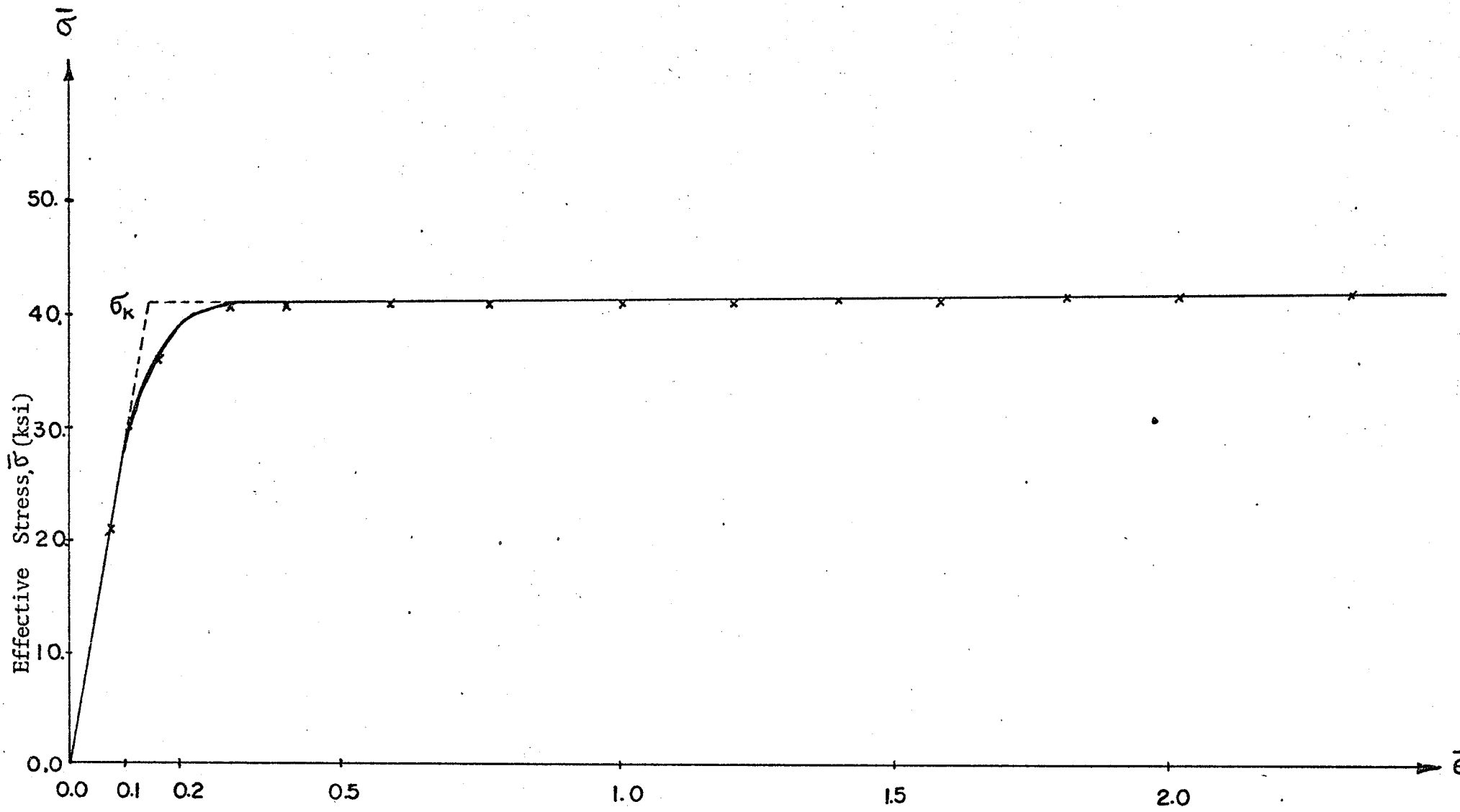

Figure 12 Effective Stress - Effective Strain Relationship Curve

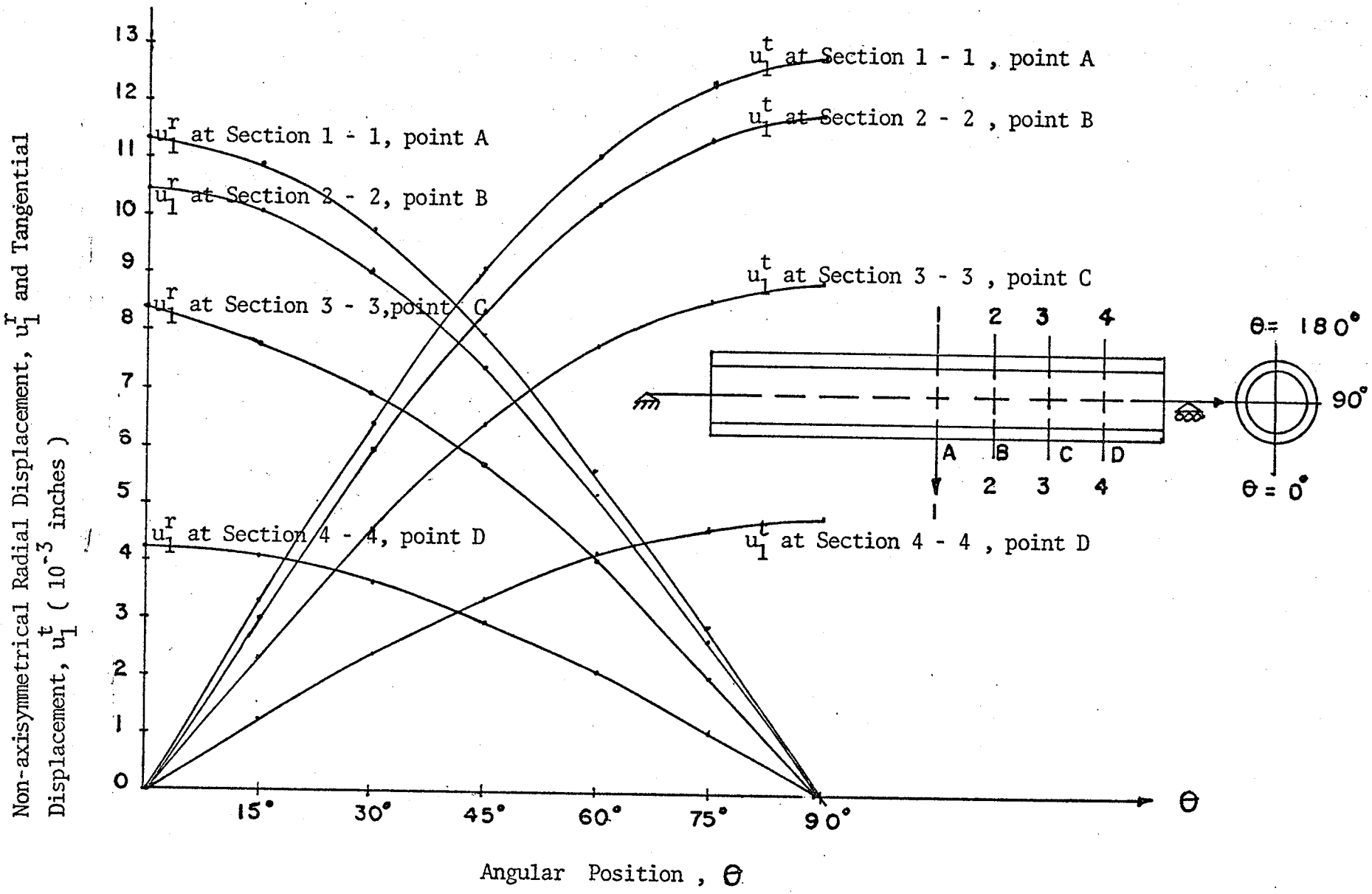

Figure 13 Radial & Tangential Displacement along Circumferential Direction at Various Sections of The Tube at $\overline{\epsilon}_{max}$ = 3.94%

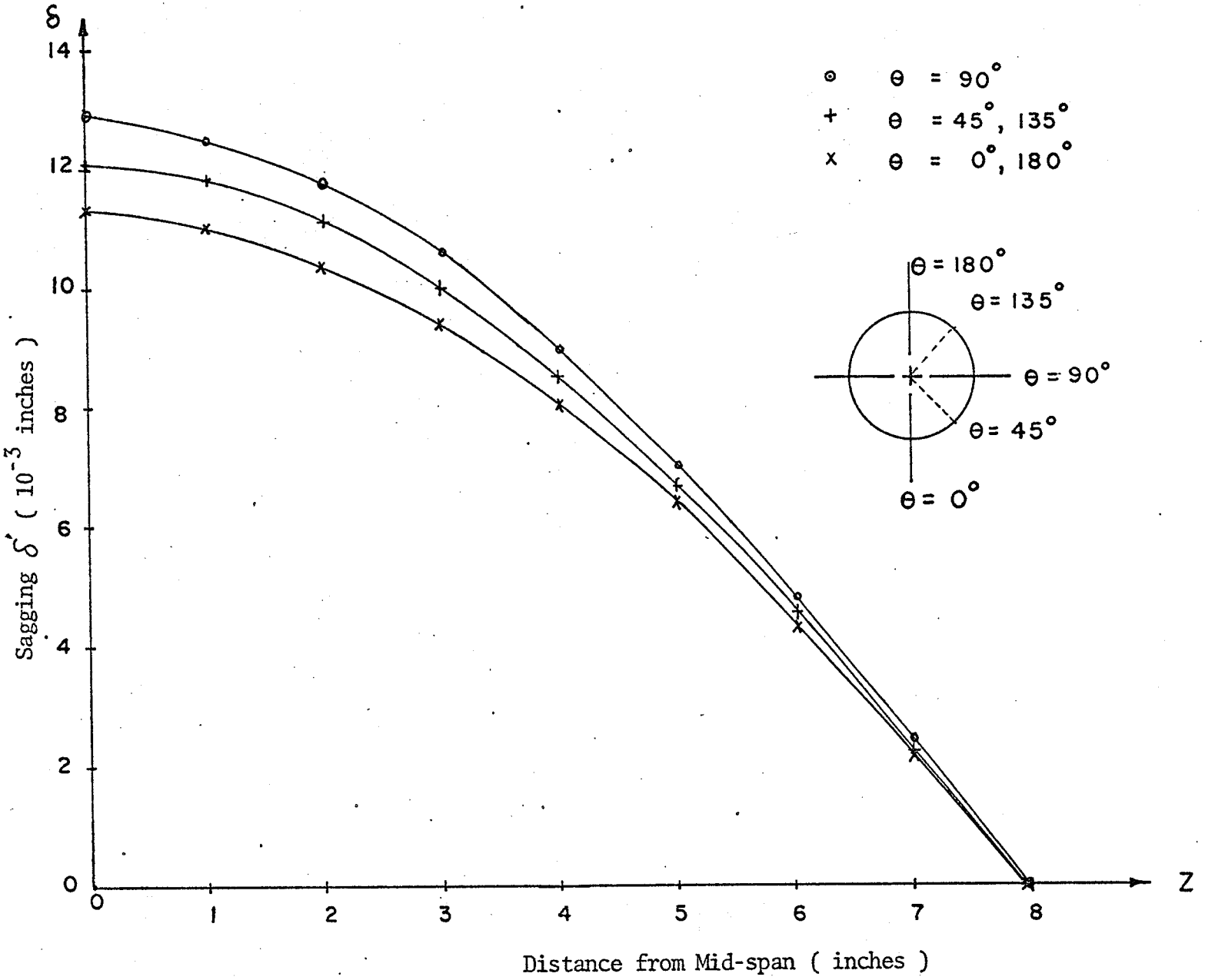

Figure 14 Sagging Along Logitudinal Direction at $\overline{\epsilon}_{max}$ = 3.94%

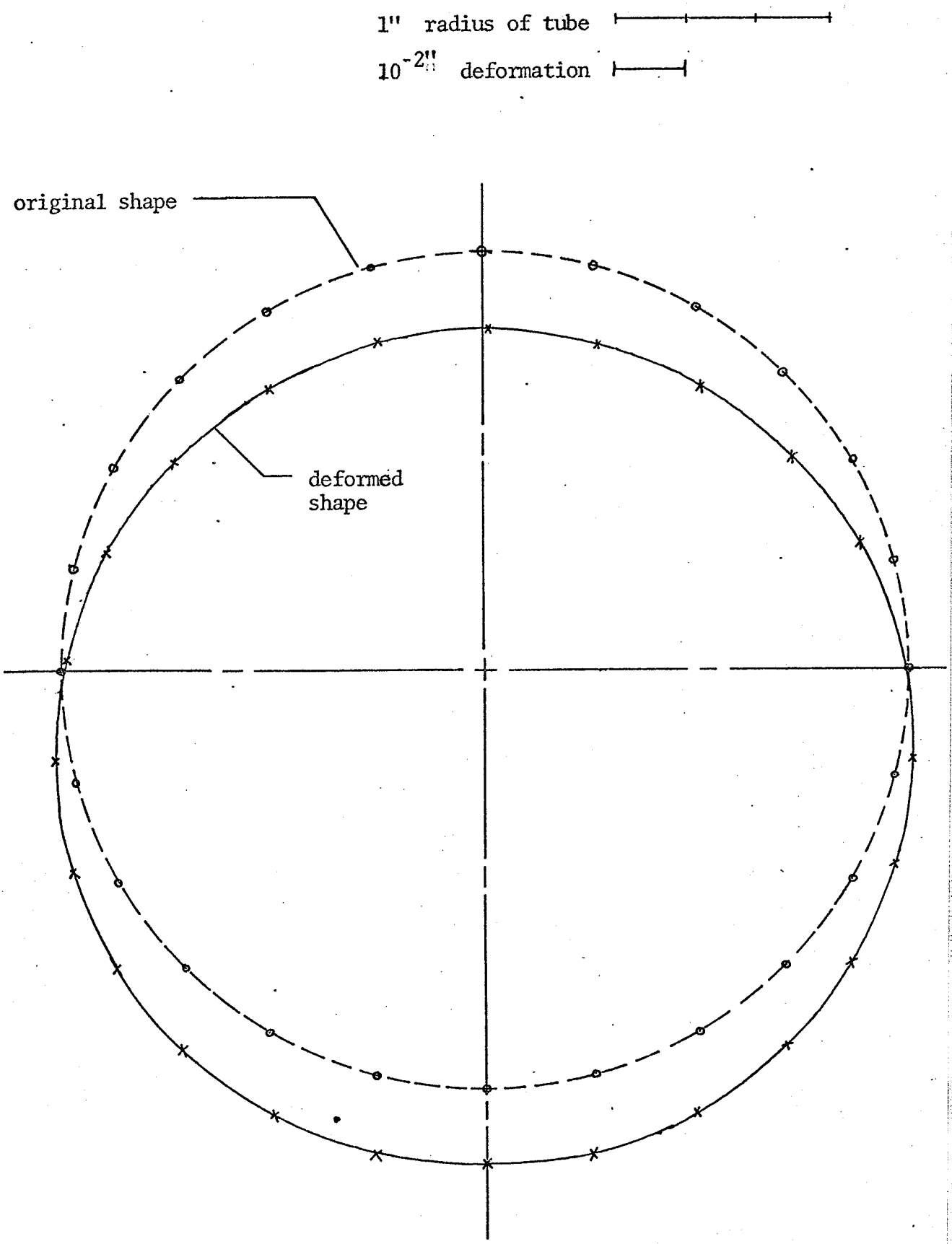

Figure 15 Deformed Shape of The Mid-span cross-section of The Tube at $\bar{\epsilon}_{max} = 3.94\%$

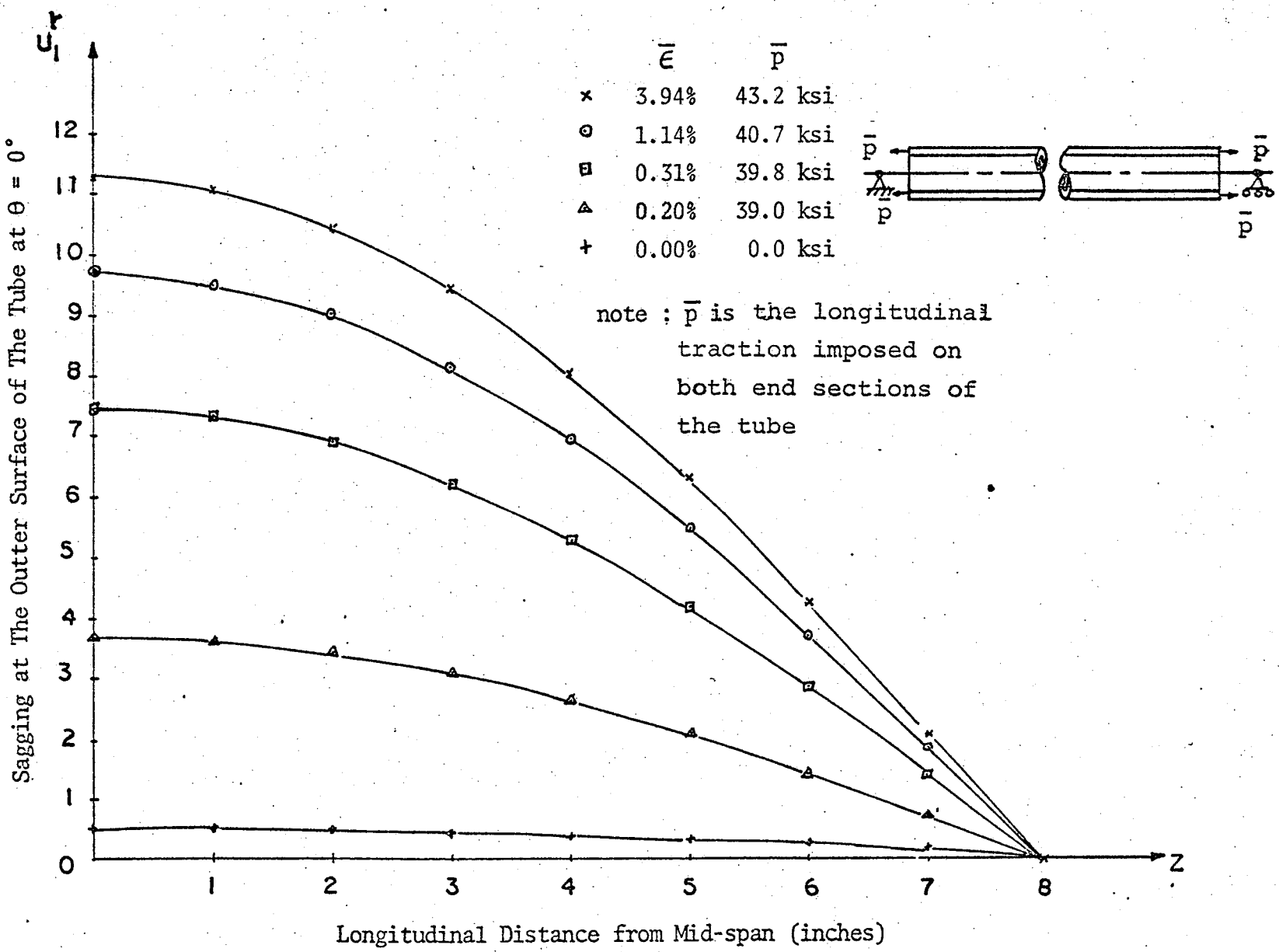

Figure 16 Sagging of The Outer Surface of The Tube at θ = 0° along Logitudinal Direction at Various States of Strain

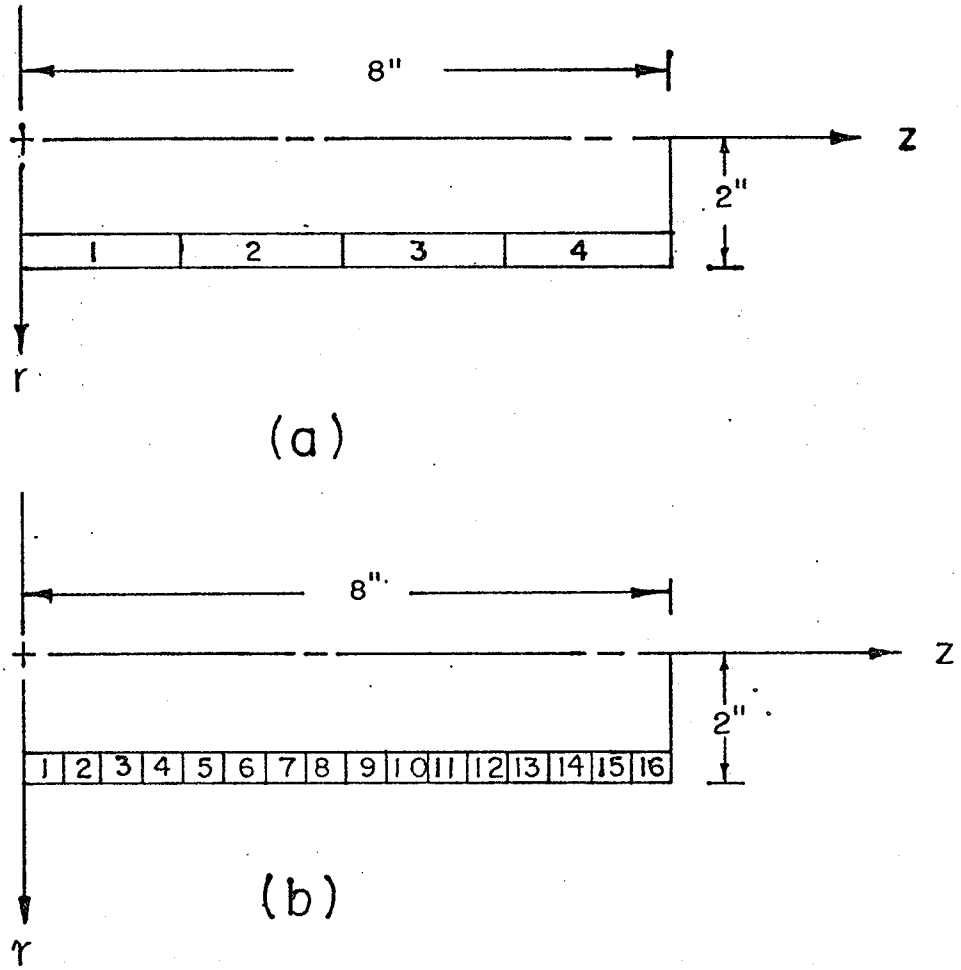

Figure 17 Finite Element Discretization of One Quarter Region of The Tube (as shown in Fig. 11-a)
(a) with 4 Elements and 10 Nodes
(b) with 16 Elements and 34 Nodes